Published in final edited form as:
J Neurosci. 2008 December 24; 28(52): 14042–14055. doi:10.1523/JNEUROSCI.4848-08.2008.

Bidirectional Hebbian Plasticity at Hippocampal Mossy Fiber Synapses on CA3 Interneurons

Emilio J Galván[1], **Eduardo Calixto**[2], and **Germán Barrionuevo**[1,*]

1*Department of Neuroscience, University of Pittsburgh, Pittsburgh, PA, USA*

2*Instituto Mexicano de Psiquiatría, Div. Inv. Neurociencias I.N.P. México City, México.*

Abstract

Hippocampal area CA3 is critically involved in the formation of non-overlapping neuronal subpopulations ("pattern separation") to store memory representations as distinct events. Efficient pattern separation relies on the strong and sparse excitatory input from the mossy fibers (MF) to pyramidal cells and feed-forward inhibitory interneurons. However, MF synapses on CA3 pyramidal cells undergo LTP, which, if unopposed, will degrade pattern separation as MF activation will now recruit additional CA3 pyramidal cells. Here we demonstrate MF LTP in stratum lacunosum-moleculare (L-M) interneurons induced by the same stimulation protocol that induces MF LTP in pyramidal cells. This LTP was NMDAR-independent, and occurred at MF Ca^{2+}-impermeable (CI) AMPAR synapses. LTP was prevented by with voltage clamping the postsynaptic cell soma during HFS, intracellular injections of the Ca^{2+} chelator BAPTA (20 mM) or bath applications of the L-type Ca^{2+} channel blocker nimodipine (10 μM). We propose that MF LTP in L-M interneurons preserves the sparsity of pyramidal cell activation, thus allowing CA3 to maintain its role in pattern separation. In the presence of the mGluR1α antagonist LY367385 (100 μM) the same HFS that induces MF LTP in naïve slices triggered NMDAR-independent MF LTD. This LTD, like LTP, required activation of the L-type Ca^{2+} channel, and also was induced following blockade of IP3 receptors with heparin (4mg/mL) or the selective depletion of receptor-gated Ca^{2+} stores with ryanodine (10 or100 μM). We conclude that L-M interneurons are endowed with Ca^{2+} signaling cascades suitable for controlling the polarity of MF long-term plasticity induced by joint pre- and postsynaptic activities.

Keywords

mossy fiber; LTP; LTD; calcium impermeable AMPARs; CA3 interneurons; feed-forward inhibition

Introduction

The circuitry of area CA3 is believed to transform neocortical inputs in a way that overlap between different activity patterns is minimized ("pattern separation") (McNaughton and Morris, 1987; Treves and Rolls, 1992; O'Reilly and McClelland, 1994; Leutgeb and Leutgeb, 2007). This pattern separation facilitates storage of distinct episodic memories and reduces recall errors. Computational models of hippocampal connectivity (Treves and Rolls, 1992) have shown that pattern separation requires parallel activation of two excitatory afferent inputs to area CA3: the perforant path (PP), the axons of stellate cells in entorhinal cortex (EC) layer

Correspondence should be addressed to: Germán Barrionuevo, Department of Neuroscience, A210 Langley Hall, University of Pittsburgh, PA. 15260; Phone: (412) 624-7330; Fax: (412) 624-9198. E-mail, german@pitt.edu.
Section and Senior Editor: Cellular/Molecular

II, and the mossy fibers (MF), the axons of dentate gyrus granule cells. The PP input is diffuse but weak, and conveys the compressed representations of neocortical activity from EC. The MF input is sparse but strong, and selects subpopulations of pyramidal cells to establish non overlapping representations via strengthening of their recurrent collateral synapses. However, the MF input innervates more interneurons than pyramidal cells (Acsady et al., 1998), and although MF synapses onto CA3 interneurons have only one or two active zones (Acsady et al., 1998), the interneuron activation from the dentate gyrus is highly effective (Henze et al., 2002). When multiple cortical input patterns to CA3 arrive simultaneously, feed-forward inhibition driven by MF will limit the number of pyramidal cells activated by the same input. This synergistic excitatory action onto feed-forward inhibitory interneurons could further increase the sparsity of the activity patterns (Mori et al., 2007), and the network storage capacity in CA3 (Treves and Rolls, 1992).

Like most cortical glutamatergic pathways, the MF input exhibits LTP at synapses on pyramidal cells in response to high-frequency stimulation (HFS) (Jaffe and Johnston, 1990; Stabubli et al., 1990; Zalutsky and Nicoll, 1990; Urban and Barrionuevo, 1996; Yeckel et al., 1999; Contractor et al., 2002). The resulting increase in pyramidal cell depolarization may promote the induction of Hebbian potentiation at their recurrent collateral synapses during the transfer and decorrelation of the compressed memory representations (Nakazawa et al., 2002). Such plasticity would allow future presentations of similar patterns to drive the same group of CA3 cells without the strong input from MF. On the other hand, an increased gain in synaptic efficacy at MF synapses on pyramidal cells would likely be accompanied by degradation in pattern separation as many more CA3 pyramidal cells are activated. If MF input to pyramidal cells and feed-forward interneurons simultaneously undergoes LTP, then the balance between excitation and inhibition is restored and the sparsity in the spatiotemporal segregation of pyramidal cell assemblies is maintained. Indeed, preservation of a narrow temporal window for synaptic integration following CA1 pyramidal cell LTP requires concurrent LTP at excitatory synapses on feed-forward interneurons (Lamsa et al., 2005). However, extensive studies on CA3 feed-forward inhibitory interneurons in the stratum lucidum have shown that the preferential form of plasticity at MF synapses is LTD (Lawrence and McBain, 2003; Pelkey and McBain, 2007; cf. Nicoll and Schmitz, 2005) which would further reduce pattern separation in the CA3 network. Given that interneuron classes in the hippocampus represent a diverse cell population (Freund and Buzsaki, 1996), the lack of MF LTP in stratum lucidum interneurons may be due to target-cell-specific differences (Kullmann and Lamsa, 2007; Pelkey and McBain, 2008). In the present study we performed a detail analysis of the mechanisms underlying the induction of long-term plasticity at MF synapses on feed-forward inhibitory interneurons with soma location in the stratum lacunosum-moleculare (L-M) of area CA3 in rat hippocampal slices.

Methods

Slice preparation

Animal use was in accordance with the University Institutional Animal Care and Use Committee. Male Sprague-Dawley rats (22 ± 4 days old; Zivic Miller Company) were deeply anaesthetized (Nembutal, IP, 5 mg/100 gr body weight) and perfused intracardially with a modified artificial cerebrospinal fluid ACSF in which sucrose substituted for NaCl (concentrations in mM): sucrose, 230; KCl, 1.9; $Na_2PO_4*7H_2O$, 1.2; $NaHCO_3$, 25.0; glucose, 10.0; $CaCl_2$, 1.0 $MgCl_2$, 4.0 at 4°C. Following 1–2 minutes of perfusion, animals were decapitated and the brains removed. Blocks of hippocampus were glued to the stage of a Leica VT1000S and cut in 350 μm-thick sections. Slices were maintained for at least 60 min in an incubation solution of the following composition (in mM): 125 NaCl, 2.0 KCl, 1.2 NaH_2PO_4, 25 $NaHCO_3$, 10 glucose, 1 $CaCl_2$ and 6 $MgCl_2$; pH 7.3 maintained with bubbled

O_2 (95%)/CO_2 (5%) at room temperature. The slices were then transferred to a submersion recording chamber and superfused at constant flow (2.5 ml/min) with the following solution (in mM): 125 NaCl, 3 KCl, 1.25 Na_2HPO_4, 25 $NaHCO_3$, 2 $CaCl_2$, 1 $MgCl_2$, 10 glucose, 0.01 (-)-Bicuculline methobromide); 0.05 D-AP5 (D-2-amino-5-phosphonopentanoic acid). The temperature of the solution in the recording chamber was set at 33 ± 1°C.

Whole-cell recordings

Interneurons were identified visually with infrared video microscopy and differential interference contrast optics. Patch pipettes were pulled from borosilicate glass and had resistances of 3–6 MΩ when filled with a solution containing (in mM), 120 K-methylsulphate, 10 NaCl, 10 KCl, 10 HEPES, 0.5 EGTA, 4.5 Mg.ATP, 0.3 Na_2.GTP, 14 phosphocreatine. Biocytin, (0.1%) was routinely added to the pipette solution to allow subsequent morphological identification and reconstruction of the interneurons (Fig. 1A, B). For BAPTA experiments, the final K-methylsulphate concentration was decreased to 75 mM and 20 mM of tetrapotassium BAPTA ($4K^+$-BAPTA; Sigma) was added. Osmolarity was routinely checked and adjusted to 295 – 300 mOsm with a pH 7.2 – 7.3.

Electrophysiological measurements of membrane properties

The membrane potential was measured immediately following cell break-in. After the cell's membrane potential was stabilized in current-clamp, a series of inward and outward current steps (500 ms duration; 30 pA increments) were injected via the whole-cell pipette to assess input resistance (Ri), action potential (AP) amplitude, and after hyperpolarization (AHP) amplitude. Ri was calculated as the slope of linear fit between voltage and injected current AHP amplitude was measured from AP threshold to the hyperpolarization peak. Experiments were analyzed only if the access resistance was <10 MΩ or it changed less than 15% of the initial value. Access resistance was monitored throughout the length of experiments.

Stimulation techniques

MF synaptic responses were evoked by extracellular stimulation using concentric bipolar electrodes (12.5 μm inner pole diameter, 125 μm outer pole diameter; FHC Inc., ME) positioned on the suprapyramidal blade of the dentate gyrus (SDG; Calixto et al., 2008; Fig. 1A). In some experiments, a second stimulating electrode was placed in the s. pyramidale of area CA3 to activate the commissural/associational (C/A) fibers. Stimulation consisted of single monopolar pulses (100 to 300 μA; 50–100 μs duration) at 0.25 Hz. To reduce the probability of antidromic activation of CA3 pyramidal cells via stimulation of their axon collaterals, we used low current intensities which resulted in composite EPSP with amplitudes less than 30% of the threshold amplitude required to evoke action potentials in the recorded interneurons. Paired pulse facilitation (PPF; 60 ms ISI) was assessed in current clamp mode. PPF was calculated as the paired pulse ratio (PPR) of the amplitude of the second EPSP to that of the first in the pair.

Identification of MF synaptic input

Current and voltage clamp recording were obtained with an Axoclamp-1D amplifier (Axon Instruments) in the presence of (-)-bicuculline methiodide (10 μM) and D-2-Amino-5-phosphonovaleric acid, D-AP5 (50 μM) to block $GABA_A$ and NMDAR-mediated responses, respectively (Supplementary table 1, summarizes the properties MF EPSPs on L-M interneurons). The group II metabotropic glutamate receptor agonist 2*S*, 2'*R*, 3'*R*)-2-(2',3'-dicarboxycyclopropyl) glycine (DCG-IV; 1 μM) was applied at the end of every experiment to confirm the MF origin of the EPSP (Fig. 1c, 1d). While DGC-IV inhibition of MF transmission in pyramidal cells is consistently complete (≥90% (Kamiya et al., 1996), it is variable in interneurons (Alle et al., 2001; Lawrence and McBain, 2003; Calixto et al., 2008).

Therefore, synaptic responses were classified as of MF origin if their DCG-IV-sensitive was >50% inhibition (Lawrence and McBain, 2003).

Criteria for LTP and LTD

LTP and LTD were induced by HFS consisting of 3 trains of 100 pulses each at 100 Hz, repeated every 10 sec paired with a postsynaptic depolarizing current step (30 ± 0.6 pA) in current clamp mode. This induction protocol produced strong postsynaptic firing. Changes in the strength of the compound EPSP were assessed by measuring the initial slope of the EPSP waveform (20–80% from the EPSP onset). Minimally evoked EPSPs and EPSCs were quantified measuring peak amplitude of the waveform. We defined LTP as stable potentiation of >25% with respect to baseline for at least 30 min post-HFS (Lamsa et al., 2005). LTD was defined as a reduction of synaptic efficacy of <25% for at least 30 min post-HFS. Values from each experiment normalized to its pre-HFS baseline magnitude for comparison across experiments. Signals were low-pass filtered at 5 kHz, digitized at 10 kHz, and stored on disk for off-line analysis. Data acquisition and analysis were performed using customized LabView programs (National Instruments, Austin TX)

Minimal stimulation techniques

These experiments were performed and analyzed as previously reported by others (Stevens and Wang, 1994; Xiang et al., 1994; Perez et al., 2001; Lawrence et al., 2004). To identify putative single MF synaptic connections, the stimulus strength was gradually reduced until no EPSPs were detected and then increased in increments of 5 μA until at an abrupt stimulation threshold where responses were reliably evoked at a failure rate between 30% and 60% (failures were identified by visual inspection). Cells were held at 69 ± 0.1 mV and access resistance was monitored every 10 min throughout the experiments. MF EPSPs were included according to the following criteria: invariant EPSPs latency and shape, and mono exponential EPSP decay. Under these conditions, we assumed that the EPSP recording was predominantly monosynaptic, and due to the activation of a single MF fiber. Minimally EPSPs were evoked at 0.25 Hz. After a 5 min stable baseline period, LTP was induced by injecting a postsynaptic depolarizing current step (30 ± 0.6 pA) that evoked action potentials when paired to the HFS train. EPSPs were recorded for at least 30 min post-HFS, and then DCG-IV was applied to confirm their MF origin.

Statistical analysis

Group measures are expressed as means ± S.E.M. To determine the statistical significance of the changes in EPSP amplitude, the mean EPSP amplitude baseline was compared to the mean EPSP amplitude at 25 – 30 min post-HFS. Normality of the populations were tested with Kolmogorov-Smirnov test ($P < 0.05$), followed by one way ANOVA and a Student-Newman-Keuls all pairwise comparisons ($P < 0.05$). In all cases differences were considered significant if P was less than alpha = 0.05. In the figures, statistical significance is denoted as follows: * $P < 0.05$, and ** $P < 0.001$ (or higher).

Drugs

D-AP5, (-)-Bicuculline methobromide, DCG-IV, LY367385 and MPEP were purchased from TOCRIS (Ellisville, MO). Philanthotoxin 433, BAPTA, Nimodipine and low-molecular-weight heparin (H-3400) were acquired from Sigma Chemical (St. Louis, MO). Purified Ryanodine was obtained from Biomol International LP.

Morphological reconstruction

Following recordings, slices were fixed in cold 4% paraformaldehyde for 72 hrs, transferred into an anti-freeze solution (one-to-one mixture of glycerol and ethylene glycol in 0.1M

phosphate buffer), and stored at −80°C. Slices were then cut into 60-μm sections on a vibratome, reacted with 1% H_2O_2 and placed in blocking serum with 0.5% Triton X-100 for 2 hrs at room temperature. Biocytin-labeled neurons were incubated with ABC-peroxidase and developed using the Ni-enhanced DAB chromogen. Interneurons were reconstructed using the Neurolucida tracing system (MicroBrightField, Inc., Williston, VT) on a Axioplan 2 Zeiss microscope equipped with DIC, a 100x (NA =1.4) planapochromatic lens and additional Optovar magnification of 1.6x (final optical magnification, 1,600x; screen magnification, 7,200x). For the reconstructions, all sections containing the cell were used.

Results

AMPAR composition of the MF synapse on L-M interneurons

Visually guided whole cell recordings in combination with biocytin cell labeling were obtained from the somata of interneurons positioned in the s. lacunosum-moleculare at about 278 ± 20 μm from the boundary between s. pyramidale and s. lucidum, 150 ± 20 μm from the SDG (Fig. 1A), and 60 to 100 μm below the slice surface. Post-hoc analysis of labeled interneurons revealed that somata were positioned at −2.45 ± 0.67 mm from bregma, and 2.33 ± 0.16 mm from midline (Ascoli et al., unpublished observations). L-M interneurons gave rise to complex axonal arbors, which extended beyond the somatic layer position into the stratum radiatum and stratum lucidum (Fig. 1A, B). Most dendritic branches exhibited a conspicuous lack of spines. Some of the dendrites branches in the s. lacunosum-moleculare course near the SDG where they could receive input from the MF axons traveling to the s. lucidum or from MF collateral plexuses in the hilus of the dentate gyrus (Claiborne et al., 1986;Acsady et al., 1998). In addition, these interneurons also may receive MF input from synapses *en passant* in the s. lucidum or from filipodial extensions arising from MF boutons on CA3 pyramidal cells in the s. pyramidale (Acsady et al., 1998). However, our previous observations suggest that MF input elicited from the SDG stimulation site is predominantly evoked from axonal projections confined to dendrites near the hilus (Calixto et al., 2008). We previously reported the passive and active membrane properties of L-M interneurons (Calixto et al., 2008).

In hippocampal pyramidal cells, AMPARs are calcium-impermeable (CI) composed of heteromeric GluR1, GluR2 and GluR3 subunits, whereas hippocampal interneurons also express GluR2-lacking calcium-permeable (CP) AMPARs (Dingledine et al., 1999; Toth et al., 2000; Bischofberger and Jonas, 2002). The GluR2-lacking AMPARs are selectively blocked by the extracellular application of the polyamine toxin philanthotoxin (PhTx). Based on the sensitivity of MF EPSPs to PhTx, L-M interneurons were classified in two subpopulations (Fig. 1F). In 18/28 cells, PhTx (5 μM) produced a small (≤10%) but significant reduction in EPSP amplitudes (93 ± 2.6% of baseline; $P < 0.05$, one way ANOVA; Fig. 1C; Supplementary table 1). EPSPs were subsequently depressed by DCG-IV (1 μM; 66.2 ± 4.6% inhibition, $P < 0.001$ one way ANOVA; Fig. 1C) confirming that they were originated from MF synapses (Toth et al., 2000; Alle et al., 2001; Calixto et al., 2008). These EPSPs were classified as produced by CI-AMPARs (Lei and McBain, 2002). In the 10 remaining cells, MF EPSP amplitudes were substantially reduced (≥50%) by PhTx (53.3 ± 8.4% of baseline; Fig. 1D, F), and further depressed by DCG-IV (63.2 ± 8% inhibition; $P < 0.001$ one way ANOVA). These MF EPSPs were categorized as originating from CP-AMPARs (Lei and McBain, 2002). These two subpopulations of interneurons appear to coexist in close proximity to each other within the stratum lacunosum moleculare. In some experiments, we also assessed the current–voltage relationship (I-V) of AMPAR EPSCs. In agreement with previous reports (Toth and McBain, 1998; Laezza et al., 1999), the PhTx insensitive AMPAR EPSCs exhibited near linear I-V relationships whereas the PhTx sensitive AMPAR EPSCs showed a strong inward rectification (Fig. 1E).

MF LTP is input specific and induced at predominantly CI-AMPAR synapses

Previous studies demonstrated that MF LTP in pyramidal cells is input specific (Zalutsky and Nicoll, 1990), and induced at synapses containing CI-AMPARs (Toth et al., 2000) in the absence of NMDAR-activation (Harris and Cotman, 1986). Given the considerable proportion of MF synapses that were weakly sensitive to the PhTx block (62%), we postulated that CI-AMPARs on L-M interneurons may be capable of supporting input-specific, NMDAR-independent MF LTP. To test this hypothesis, MF EPSCs and commissural/associational (C/A; Fig. 1A) EPSCs were recorded simultaneously (V_h = 69 ± 3 mV) in the presence of PhTx (5 μM) in perfusion bath. In 11/18 cells (61% of total), PhTx modestly reduced MF EPSC amplitudes (93.5 ± 3% of baseline; $P < 0.05$, one way ANOVA; Figs. 2A, C) but did not affect C/A EPSC amplitudes (97.2 ± 8% of baseline, $P > 0.5$, one way ANOVA; Fig. 2A, C). At the end of the PhTx application, HFS was delivered to the MF input. The depolarized interneuron fired a train of action potentials during each of the HFS trains. Following the HFS, the isolated CI-AMPAR component of the MF EPSC exhibited a robust posttetanic potentiation (PTP; 203.3 ± 6.4% of baseline) followed by a sustained LTP (163.1 ± 17% of baseline at 30 min post-HFS; $P < 0.001$, one way ANOVA; N =11). Bath application of DCG-IV (1 μM) confirmed that the EPSCs were generated by MF synapses (67.3 ± 10.8% inhibition; Fig. 2B, C). In contrast, C/A EPSCs were not affected by the HFS of MF (95 ±10.5% at 1 min post-HFS, and 95.2 ± 16% at 30 min post-HFS; $P > 0.5$, one way ANOVA; N =11), and were insensitive to DCG-IV (3.4 ± 12.4% inhibition; Fig. 2A, B, C). Collectively these data indicate that MF LTP in L-M interneurons is input specific, and not the consequence of contamination from NMDAR-independent LTP at C/A synapses on the recorded cell. Additional data obtained in our laboratory show that similar HFS delivered to the C/A input to L-M interneurons in the presence of D-AP5 induced LTD (57.2 ± 6.8% of baseline; N = 3; Perez-Rosello and Barrionuevo, unpublished observations).

In 7/18 interneurons treated with PhTx, MF EPSCs were substantially reduced (53.3 ± 8.4% of baseline) and classified as predominantly containing CP-AMPARs. Following HFS, the isolated CI-AMPAR-mediated responses in 5/7 cells (28%) exhibited a smaller PTP (135.5 ± 15.7% relative to PhTx baseline; $P< 0.002$), and remained unchanged at 30 min post-HFS (95.9 ± 6%) despite strong postsynaptic firing during the HFS (Supplemental Fig. 1). In the remaining 2 interneurons (11%), the isolated CI-AMPAR-mediated MF EPSC underwent LTD (73.7 ± 8.2% at 30 min post-HFS; $P < 0.0001$, unpaired t-test; Supplemental Fig. 2).

We further characterize the magnitude and time-course of MF LTP in L-M interneurons in current clamp conditions (Vm = 69.6 ± 1 mV; Supplemental Table 1). In the majority of these cells (25/32; 78%), the initial slope of the MF EPSP showed robust PTP (202.8 ± 17% of baseline) followed by a sustained LTP (160.6 ± 19% at 30 min post-HFS; N = 25/32; $P < 0.001$, one way ANOVA; Fig. 3A, B, C). DCG-IV subsequently reduced the EPSP slopes by 64.7 ± 4% ($P < 0.001$; one way ANOVA). We also measured PPR during baseline (1.73 ± 0.05), at 1 min post-HFS (1.52 ± 0.03; one way ANOVA, $P < 0.001$), and at 30 min post-HFS (1.48 ± 0.04; one way ANOVA, $P < 0.05$; Fig. 2D). The reduction in PPF during LTP is suggestive of a presynaptic expression of MF LTP in L-M interneurons, as previously shown for MF LTP in pyramidal cells (Staubli et al., 1990; Zalutsky and Nicoll, 1990; Xiang et al., 1994; Sokolov et al., 2003), and dentate gyrus basket cells (Alle et al., 2001). In the remaining 7 cells, MF EPSP slopes remained unchanged post-HFS (N=5; 16% of total) or underwent LTD (N=2; 6% of total).

LTP of minimally-evoked MF EPSPs

Another a possible source of interpretational error is that the potentiation observed in L-M interneurons may have resulted from the recruitment of additional CA3 pyramidal cells because of the parallel induction of MF LTP in CA3 pyramidal cells. Hence, HFS potentiated the MF

input and also the synaptic drive from the polysynaptic recurrent collateral input. To reduce the likelihood of polysynaptic contamination, we examined changes in synaptic efficacy evoked by minimal stimulation (Fig. 4A), which putatively activates single axons that terminate onto L-M interneurons (Stevens and Wang, 1994;Xiang et al., 1994;Perez et al., 2001;Lawrence et al., 2004). During baseline period, minimal stimulation elicited MF EPSPs with average amplitudes of 0.66 ± 0.02 mV (failures included). HFS was paired with a postsynaptic depolarizing current pulse (30 ± .6 pA), and in all cases the cells fired action potentials in response to the HFS (Fig. 4B, inset). This pairing protocol yielded a sustained increase in EPSP amplitude in 6/9 cells (1.10 ± 0.03 mV at 25–30 min post-HFS; $P < 0.001$; one way ANOVA; Fig. 4B, C), and no change in the remaining 3 cells (0.64 ± 0.07 mV). LTP induced with the minimal stimulation protocol was associated with a decrease in both failure rate (30–65% during baseline; 8–30% at 25–30 min post-HFS) and coefficient of variation (CV; 0.7 ± 0.06 during baseline; 0.5 ± 0.05 at 25–30 min post-HFS; N = 6; $P < 0.02$, one way ANOVA; Fig. 4D, E, F). After 30 min of sustained LTP, the application of DCG-IV (1 μM) decreased EPSP amplitude to 0.45 ± 0.03 mV (N = 6), and increased the failure rate by 45–60%. Together these data indicate that LTP was induced directly at MF synapses on L-M interneurons, and resulted from an increase in the probability of transmitter release from MF presynaptic terminals.

MF LTP requires postsynaptic depolarization and calcium elevation

To test the involvement of postsynaptic activation in the induction of LTP, we applied HFS to MF while simultaneously voltage clamping the cell's membrane potential at −100 mV to prevent postsynaptic spiking (Fig. 5A, inset). Under these conditions, no significant changes post-HFS were detected in the EPSP slope compared to baseline responses (98.7 ± 8% at 5 min post-HFS; $P > 0.05$; 102 ± 6% at 15 min post-HFS, $P > 0.05$, N = 10; Fig. 5A). A subsequent HFS applied in current-clamp mode (Vm = 69 ± 3 mV) elicited a pronounced and sustained increase in the initial EPSP slope (165.7 ± 19% at 30 min post-HFS; N = 6; Fig. 4A, B, C; $P < 0.001$, one way ANOVA). Application of DCG-IV inhibited the initial slope of the potentiated EPSPs by 64.6 ± 6% (Fig. 5A, C).

It has been shown that elevation of postsynaptic Ca^{2+} influx is a necessary condition for the induction of MF LTP in pyramidal cells (Jaffe and Johnston, 1990; Yeckel et al., 1999; Sokolov et al., 2003; but see Zalutsky and Nicoll, 1990), and basket cells in the dentate gyrus (Alle et al., 2001). To investigate whether MF LTP in L-M interneurons depends on a rise in postsynaptic [Ca^{2+}] elicited by the HFS, the patch pipette was filled with a internal solution containing the fast calcium chelator 1, 2-Bis(2-aminophenoxy)ethane-*N*,*N*,*N'*,*N'*-tetraacetic acid, (BAPTA; 20 mM). BAPTA loading did not significantly affect the EPSP kinetics during the baseline period (Supplementary table 1), but significantly reduced the area of the Ca^{2+} dependent after-hyperpolarization potential (AHP) following trains of action potentials (77.4 ± 4.6% of baseline; $P < 0.000$, unpaired t test; N = 10; Fig. 6B). BAPTA loading did not affect PTP of the EPSP slope (202.8 ± 16.9% in control cells; N = 31; 216.3 ± 42.3% in BAPTA loaded cells; $P > 0.05$, one way ANOVA; N =11) but prevented LTP induction in 11/15 cells (96.9 ± 14% at 5 min, $P > 0.05$; 90.4 ± 11% at 30 min post-HFS, $P > 0.05$, one way ANOVA; Fig. 6A, C). The application of DCG-IV (1 μM) confirmed the MF origin of the EPSPs (62 ± 9% inhibition, $P < 0.001$, one way ANOVA; Fig. 6A, C). In the remaining 4 cells, BAPTA loading failed to block LTP (159.5 ± 8.6% of baseline at 30 min post-HFS; $P < 0.001$, unpaired t-test; 66.2 ± 2.57% inhibition by DCG-IV; data not shown). It has been reported that in pyramidal cells, block of MF LTP induced with similar HFS trains requires 30 to 50 mM BAPTA concentrations (Yeckel et al., 1999). Failure to prevent LTP in some L-M interneurons loaded with 20 mM BAPTA may indicate that some accumulation of Ca^{2+} ions took place near the Ca^{2+} sensor that triggers LTP (see Discussion).

MF LTP requires L-type Ca^{2+} channel activation

On the basis of the findings described above, we hypothesized that the induction of MF LTP in L-M interneurons requires postsynaptic Ca^{2+} influx via voltage-gated channels. It has been shown that activation of the L-type Ca^{2+} channel is necessary for the induction of NMDAR-independent forms of LTP in the hippocampus (Grover and Teyler, 1992; Kullmann et al., 1992; Huang and Malenka, 1993; Chen et al., 1998; Kapur et al., 1998; Lauri et al., 2003), and amygdala (Weisskopf et al., 1999). These data are compatible with the observations that L-type channels are abundantly expressed on the proximal dendrites and soma of hippocampal pyramidal cells and interneurons (Ahlijanian et al., 1990; Westenbroek et al., 1990), and capable of producing considerable increases in cytosolic Ca^{2+} (Miyakawa et al., 1992; Denk et al., 1996). To test whether L-type channel activation is required for MF LTP induction in L-M interneurons, the L-type channel antagonist nimodipine (10 μM) was added to the perfusion bath before the delivery of HFS. We found that nimodipine did not alter the properties of the evoked MF EPSPs (Supplementary table 1) but prevented LTP of the EPSP slope (98.4 ± 9% at 5 min $P > 0.05$, and 106.7 ± 10% at 30 min post-HFS; $P > 0.05$; $N = 9$; Fig. 7A, C). In three of these cells, we assessed the effect of nimodipine on the isolated CI-AMPAR component by including PhTx (5 μM) in the perfusion bath before HFS. In voltage clamp conditions ($V_h = -70$ mV), PhTx moderately reduced MF EPSC amplitudes (91.2 ± 4% of baseline; $P < 0.001$, unpaired t-test; Figs. 7B). At the end of the PhTx application, recording was switched to current clamp conditions (−70 mV) and HFS was delivered to the MF input. Following the HFS, the isolated CI-AMPAR component of the MF EPSP exhibited PTP (154.8 ± 6.5% of baseline) but did not show LTP (110.8 ± 6% of control at 30 min post-HFS; $P>0.5$; one way ANOVA). Bath application of DCG-IV (1 μM) confirmed that the EPSCs were generated by MF synapses (66.1 ± 4.4% inhibition; Fig. 7B). We also examined the effect of L- type channel blockade on the maintenance of LTP by adding nimodipine 10 min after the delivery of the HFS. The results of these experiments indicated that nimodipine did not affect the potentiated MF EPSP slope (169.6 ± 10% at 30 min post-HFS, $P < 0.001$; $N = 5$; Fig. 7A, C). In both cases, DCG-IV applied at the end of the experiments reduced the responses (59 ± 5% and 60.3 ± 2% with nimodipine before and after, respectively; $P < 0.001$, one way ANOVA; Fig. 7A). Together, these findings show that the induction but not the maintenance of LTP at MF synapses on L-M interneurons required the activation of L-type channels.

Blockade of mGLuR1α, IP3 receptors or ryanodine receptors results in MF LTD

The group I mGluRs (mGluR1/mGluR5) are expressed in the periphery of the postsynaptic densities in the s. lacunosum moleculare of area CA1 (Lujan et al., 1996). In particular, the mGluR1α isoform is mainly located postsynaptically in GABA-containing interneurons (Baude et al., 1993; Ferraguti et al., 2004), and is required for LTP induction in CA1 alveus/oriens interneurons (Lapointe et al., 2004; Topolnik et al., 2006). To investigate whether mGluR1α activation is also involved in the induction of MF LTP in L-M interneurons, HFS was applied in the presence of the selective antagonist (1)-2-methyl-4-carboxyphenylglycine (LY367385; 100 μM). Although PTP was similar to baseline (173 ± 7%), the same HFS protocol that induces MF LTP in naïve slices induced MF LTD in LY367385 treated slices (73 ± 12% at 30 min post-HFS; $P < 0.001$; $N = 11$; 66.8 ± 4.5% inhibition by DCG-IV; $P < 0.001$; one way ANOVA; Fig. 8A). We also tested the effect of LY367385 on the isolated CI-AMPAR component by applying PhTx (5 μM) to the perfusion bath before HFS. In voltage clamp conditions ($V_h = -70$ mV), PhTx modestly reduced MF EPSC amplitudes (95.4 ± 3% of baseline; $P < 0.05$, unpaired t-test; Figs. 8B). At the end of the PhTx application, recordings were switched to current clamp conditions (−70 mV) prior to the delivery of HFS to MF. Following a robust PTP (165.6 ± 1%), MF EPSPs underwent a pronounced LTD (71 ± 3.6 at 30 min post-HFS; $P < 0.001$; $N = 3$), and were further inhibited by DCG-IV (69.3 ± 9.1% of control).

To determine the locus of LTD expression, we examined the percentage of failures and CV using a minimal stimulation protocol. In the presence of LY367385, HFS paired with a postsynaptic depolarization pulse (~33 pA) resulted in a depression of MF EPSP amplitudes (0.55 ± 0.09 mV in baseline; 0.41 ± 0.06 mV at 25–30 min post-HFS; $P < 0.05$ one way ANOVA; N = 5; Supplementary Fig. 3A, B). The EPSP depression was associated with an increase in the failure rate (35–65% during baseline; 60–80% at 25–30 min post-HFS, $P < 0.001$ one way ANOVA; Supplementary Fig. 3C) and increase in the CV (0.6 ± 0.08 during baseline, 0.89 ± 0.08 at 25–30 min post-HFS; $P < 0.001$, one way ANOVA; N = 5; Supplementary Fig. 1D;). After 30 min of LTD, the application of DCG-IV (1 μM) decreased EPSP amplitude to 0.33 ± 0.02 mV ($P < 0.01$; N = 4, Supplementary Fig. 3A, B), and increased the failure rate by 55–90% ($P < 0.001$; one way ANOVA, Supplementary Fig. 3C, D). These data indicate that MF LTD, like MF LTP, is presynaptically expressed. In contrast to the marked effects on synaptic plasticity mediated by the mGluRlα, application of the mGluR5 selective antagonist 2-methyl-6-(phenylethynyl)-pyridine hydrochloride (MPEP; 25 μM) did not affect the polarity of synaptic plasticity induced by MF HFS (172 ± 16% at 30 min post-HFS; $P < 0.001$; one way ANOVA; N = 10; DCG-IV sensitivity = 64.5 ± 3% of baseline; $P < 0.05$; Supplementary Fig. 4).

Activation of mGluRlα is known to increase L-type Ca^{2+} channel conductance, and Ca^{2+} release from intracellular stores in the endoplasmic reticulum (ER) (Chavis et al., 1996; Woodhall et al., 1999; Fagni et al., 2000; Ouardouz et al., 2003; Bardo et al., 2006) via stimulation of the inositol (1,4,5)-trisphosphate receptor (IP3R). To test the involvement of the IP_3-IP_3R cascade initiated during the induction of MF LTP, we loaded the cells with heparin (4 mg/mL), an antagonist of IP3Rs (Taylor and Broad, 1998). The dialysis with heparin did not affect PTP (155.9 ± 8.3%) but resulted in MF LTD (76.9 ± 5.7% at 30 min post-HFS, N = 8, $P < 0.001$, one way ANOVA, and 76.1 ± 4.7% inhibition by DCG-IV; $P < 0.001$; one way ANOVA; Fig. 9A, B, C).

The rise in $[Ca^{2+}]_i$ due to activation of L-type channel and IP3 receptors could result in Ca^{2+}-induced Ca^{2+} release (CICR) from the ER via activation of the ryanodine receptor (RyR) (Wang et al., 1996; Balschun et al., 1999; Nakamura et al., 2000; Lu and Hawkins, 2002; Raymond and Redman, 2002; Morikawa et al., 2003; Sokolov et al., 2003; Tozzi et al., 2003; Lapointe et al., 2004; Mellentin et al. 2007). In dentate gyrus and CA3 hippocampal cells, RyR levels are higher than IP3R levels (Bardo et al., 2003). Furthermore, a recent study has shown that the distribution of RyR isotype 3 immunoreactivity is strong in the s. lacunosum-moleculare (Hertle and Yeckel, 2007). To examine whether blockade of the RyR also may induce LTD, ryanodine was included in the whole-cell pipette (10 μM; N =4 or 100 μM; N =4). Because both concentrations produced the same effect, the data were pooled for statistical analysis. Following PTP (176 ± 15%), MF EPSP slopes decayed to a stable LTD (75 ± 4.3% at 30 min post-HFS; N = 8; $P < 0.001$; 75.2 ± 2.4% inhibition by DCG-IV; $P < 0.001$; one way ANOVA; Fig. 9A, B, C). Together these results would suggest that the dynamic regulation of $[Ca^{2+}]_i$ by the interaction between IP3R and RyR (Nash et al., 2002) determines the balance between MF LTP and LTD (Fig. 11).

MF LTD induced by blockade of mGLuR1α requires Ca^{2+} influx through L-type channel

The lack of long-term changes at MF synapses in the presence of nimodipine (Fig. 7) suggests that LTD, like LTP, also depends on Ca^{2+} influx through the L-type channel. In the hippocampus, NMDAR independent forms of LTD have been shown to be dependent on L-type Ca^{2+} activation (Christie and Abraham, 1994;Christie et al., 1997; Wang et al., 1997). We hypothesized that in the absence of the mGluR1α signal transduction cascade, the source for $[Ca^{2+}]_i$ increase responsible for LTD is through the L-type channels. Indeed, we found that HFS applied in the presence of LY367385 (100 μM) and nimodipine (10 μM) did not change

the MF EPSP slope (92 ± 7.3% of control at 30 min post HFS; N =10; P> 0.216, paired t-test; Fig. 10). After 30 min post HFS, DCG-IV reduced the EPSP slope by 68.5 ± 7.4% of control (P<0.0001, unpaired t-test).

Discussion

Previous reports have established that LTD mediated by CP-AMPAR or NMDAR is the preferential form of long-term plasticity at MF synapses on stratum lucidum interneurons (Maccaferri et al., 1998; Toth and McBain, 1998; Toth et al., 2000; Lei and McBain, 2002). Here we demonstrate that the majority of L-M interneurons (78%) recorded near the SDG exhibit robust PTP and input-specific NMDAR-independent LTP at predominantly CI-AMPAR MF synapses. These observations support the notion that the induction of pathway-specific LTP does not require dendritic spines (Lamsa et al., 2005). By contrast, in the majority of PhTx sensitive MF synapses, the isolated CI-AMPAR component showed a reduced PTP and were unaffected by HFS. Only in few of the CP-AMPAR synapses, the CI-AMPAR-mediated EPSP exhibited a lack of PTP followed by LTD. Given that the AMPAR sensitivity to PhTx was not assessed in every experiment, the generality of our conclusion that only synapses predominantly containing CI-AMPARs are able to undergo MF LTP remains to be determined.

The axons of L-M interneurons branch in strata lacunosum-moleculare, radiatum and pyramidale, and make direct symmetrical synaptic contacts with pyramidal cells (Kunkel et al., 1988) that provide feed-forward inhibition to pyramidal cells (Lacaille and Schwartzkroin, 1988; Williams et al., 1994; Vida et al., 1998). Therefore, our results are consistent with the claim that LTP occurs at excitatory inputs to GABAergic interneurons inhibiting principal cells in a feed-forward manner (Kullmann and Lamsa, 2007). We also found that MF synapses on L-M interneurons are bi-directionally modifiable. LTP induction required the joint activation of L-type Ca^{2+} channels and mGluRlα receptors. During blockade of mGluRlα, the same stimulation protocol that induces MF LTP in naï;ve slices induced MF LTD. The requirement for conjunctive pre- and postsynaptic activity to induce both LTP and LTD fulfills the condition for Hebbian forms of synaptic plasticity.

To ensure that MF LTP in L-M interneurons is not due to the induction of NMDAR-independent LTP at polysynaptic recurrent synapses from intercalated pyramidal cells, we first systematically identified MF EPSPs based on their differential sensitivity to DCG-IV. Second, we explicitly tested the lack of C/A LTP by applying HFS to C/A fibers in the absence of NMDAR activation. Third, LTP was detected with a minimal stimulation protocol during which only one or a few synapses were activated (Stevens and Wang, 1994; Xiang et al., 1994; Perez et al., 2001). Finally, LTP was prevented with somatic voltage clamping during HFS, and by intracellular injections of the Ca^{2+} chelator BAPTA. Together these data clearly show that MF LTP was induced postsynaptically and expressed directly at MF synapses on L-M interneurons.

MF synapses onto interneurons are made either by small *en passant* varicosities originating from the axon trunks of MF traveling in the s. lucidum of CA3, or from dentate gyrus hilar collaterals or filipodial extensions from the large synaptic boutons innervating the pyramidal cells (Claiborne et al., 1986; Acsady et al., 1998; Bischofberger and Jonas, 2002). In contrast, MF synapses on pyramidal cells have large presynaptic boutons with small finger-like extensions (Hamlyn, 1962; Amaral, 1979). Despite significant morphological differences in presynaptic terminals, MF synapses on pyramidal cells and the subpopulation of L-M interneurons containing MF CI-AMPARs share some similarities in the mechanisms of synaptic transmission and use dependent plasticity. Pyramidal cells, which are predominantly innervated by MF at CI-AMPAR-containing synapses (Toth et al., 2000), exhibit robust PTP

and LTP, and LTP is induced postsynaptically (Jaffe and Johnston, 1990; Yeckel et al., 1999; Contractor et al., 2002; Sokolov et al. 2003; but see Zalutsky and Nicoll, 1990). However, the PTP and LTP reported here are comparatively smaller than the PTP and LTP at MF synapses made by the axon collaterals of granule cells on basket cells in the dentate gyrus (Alle et al., 2001). On the other hand, MF LTP in these interneurons was only partially attenuated by BAPTA, indicating that the induction mechanisms are more resilient to chelation of postsynaptic Ca^{2+} than those underlying LTP induction in L-M interneurons.

Both LTP and LTD were prevented by nimopidine applications prior to HFS. An essential role of L-type channels in long-term synaptic plasticity in CA3 interneurons has not previously been demonstrated. Our results also indicate that mGluRlα serves as a molecular switch that changes the outcome of the synaptic modification triggered by activation of L-type Ca^{2+} channels (Fig. 11). Activation of this switch by glutamate release results in LTP induction; however, if the switch is inoperative LTD is triggered by the Ca^{2+} influx through activation of the L-type channel following the postsynaptic depolarization mediated by CI-AMPA receptor activation (Fig. 11). These findings would be consistent with the idea that the magnitude of the activity-dependent rise in postsynaptic Ca^{2+} is a major determinant of the direction of change in synaptic efficacy (Bear et al., 1987;Artola and Singer, 1993;Hansel et al., 1997;Cormier et al., 2001). Experimental observations suggest that the induction threshold for LTP requires higher levels of postsynaptic $[Ca^{2+}]_i$ than for LTD (Cummings et al., 1996;Cho et al., 2001;Nevian and Sakmann, 2006). Therefore, LTP at MF synapses onto L-M interneurons may only be induced following an increase in the L-type channel conductance (Chavis et al., 1996) supplemented by Ca^{2+} mobilization via IP3R, and RyR-mediated CICR (Nakamura et al., 2000;Fig. 11). However, LTP may not depend solely on global $[Ca^{2+}]_i$ but on a separate Ca^{2+} sensor (Karmarkar and Buonomano, 2002;Bender et al., 2006;Nevian and Sakmann, 2006), enabled by mGluRlα activation. Another obligatory step in the downstream signaling cascade leading to MF LTP may involve the activation of PKA and PKC (Galvan and Barrionuevo, unpublished observations). In turn, PKC activation could mediate a phosphorylation-triggered desensitization of mGluRlα (Dale et al., 2002;Sato et al., 2004) perhaps via coactivation of mGluR5 (Poisik et al., 2003), which would prime potentiated MF synapses for a subsequent induction of LTD. Such metaplasticity (Abraham and Bear, 1996) could provide with a homeostatic mechanism to reset synaptic weights and prevent synaptic saturation (Turrigiano and Nelson, 2004) at MF synapses on L-M interneurons.

Previous reports have demonstrated that MF synapses on lucidum interneurons and dentate gyrus basket cells are able to undergo bidirectional plasticity. However, the mechanism that regulates the polarity of synaptic efficacy in these interneuron populations is different from that reported here. In lucidum interneurons where MF LTD at naïve synapses requires presynaptically located mGluR7 activation, HFS elicited MF LTP/dedepression only after L-AP4 applications induced chemical LTD and internalization of mGluR7 localized at MF terminals (Pelkey et al., 2005). The requirement for strong presynaptic receptor activation to elicit LTP indicates that this synaptic plasticity is more suitable for maintaining network stability during sustained activation of granule cells (for e.g., during epileptic bursting) (Pelkey et al., 2005). In dentate gyrus basket cells, MF synapses can exhibit either LTP or LTD depending on the postsynaptic membrane potential during HFS (Alle et al., 2001).

While many mechanisms for NMDAR-independent LTP/LTD have been described in hippocampal interneurons, the expression of this plasticity appears solely determined by changes in transmitter release probability (Kullmann and Lamsa, 2007). Indeed, the changes in PPR, coefficient of variation and failure rate that were detected during MF LTP/LTD are all indicative of a presynaptic locus of expression for the changes in synaptic efficacy. Presynaptic changes at MF synapses on pyramidal cells and interneurons have been previously reported during both LTP (Staubli et al., 1990; Zalutsky and Nicoll, 1990; Xiang et al., 1994; Alle et

al., 2001), and LTD (Domenici et al., 1998; Lei and McBain, 2002). We speculate that the postsynaptic events in response to HFS are expressed presynaptically by a retrograde signaling messenger.

Functional Implications

According to computational and behavioral studies on hippocampal function (McNaughton and Morris, 1987; Treves and Rolls, 1992; O'Reilly and McClelland, 1994; Lisman, 1999; Leutgeb et al., 2007), the strong and sparse input from the MF input selects non overlapping subpopulations of pyramidal cells to encode new memory representations in a way that reduces interference between stored information. Feed-forward inhibitory interneurons also may play a role in regulating the transfer and decorrelation of the compressed memory representation in area CA3. For example, the parallel activation of feed-forward inhibitory interneurons by MF could contribute to pattern separation by restricting the temporal window for synaptic integration and action potential firing in pyramidal cells (Pouille and Scanziani, 2001; Perez-Orive et al., 2002). Therefore, the fine “tuning” of the pyramidal cell network during pattern separation requires a functional balance between monosynaptic excitation and disynaptic inhibition (Marino et al., 2005). If MF LTP were confined to synapses on pyramidal cells alone, this could limit the sparseness of the memory representation unless it is accompanied by a compensatory LTP on feed-forward inhibitory interneurons (Lamsa et al., 2005). The present results demonstrate that the feed-forward inhibitory drive to CA3 mediated by the MF input to L-M interneurons has the ability to undergo Hebbian LTP in response to the same stimulation protocol that induces MF LTP in pyramidal cells (cf. Henze et al., 2000; Nicoll and Schmitz, 2005). Similar strengthening of MF connections on both postsynaptic targets by the same presynaptic activity could contribute to preserve the focus of the excitatory drive from the dentate gyrus to the CA3 neuronal network. This would presumably be important for invoking a distributed encoding that minimizes the overlap between incoming cortical patterns that underlie different memory representations.

Supplementary Material

Refer to Web version on PubMed Central for supplementary material.

Acknowledgements

We thank John Cavaretta for their help with the interneuron reconstruction and technical support. This work was supported by NINDS grant NS24288

References

Abraham WC, Bear MF. Metaplasticity: the plasticity of synaptic plasticity. Trends Neurosci 1996;19:126–130. [PubMed: 8658594]

Acsady L, Kamondi A, Sik A, Freund T, Buzsaki G. GABAergic cells are the major postsynaptic targets of mossy fibers in the rat hippocampus. J Neurosci 1998;18:3386–3403. [PubMed: 9547246]

Ahlijanian MK, Westenbroek RE, Catterall WA. Subunit structure and localization of dihydropyridine-sensitive calcium channels in mammalian brain, spinal cord, and retina. Neuron 1990;4:819–832. [PubMed: 2163262]

Alle H, Jonas P, Geiger JR. PTP and LTP at a hippocampal mossy fiber-interneuron synapse. Proc Natl Acad Sci U S A 2001;98:14708–14713. [PubMed: 11734656]

Amaral DG. Synaptic extensions from the mossy fibers of the fascia dentata. Anat Embryol (Berl) 1979;155:241–251. [PubMed: 453543]

Artola A, Singer W. Long-term depression of excitatory synaptic transmission and its relationship to long-term potentiation. Trends Neurosci 1993;16:480–487. [PubMed: 7507622]

Balschun D, Manahan-Vaughan D, Wagner T, Behnisch T, Reymann KG, Wetzel W. A specific role for group I mGluRs in hippocampal LTP and hippocampus-dependent spatial learning. Learn Mem 1999;6:138–152. [PubMed: 10327239]

Bardo S, Cavazzini MF, Emptage N. The role of the endoplasmic reticulum Ca^{2+} store in the plasticity of central neurons. Trends Neurosci 2006;27:78–84.

Baude A, Nusser Z, Roberts JD, Mulvihill E, McIlhinney RA, Somogyi P. The metabotropic glutamate receptor (mGluR1 alpha) is concentrated at perisynaptic membrane of neuronal subpopulations as detected by immunogold reaction. Neuron 1993;11:771–787. [PubMed: 8104433]

Bear MF, Cooper LN, Ebner FF. A physiological basis for a theory of synapse modification. Science 1987;237:42–48. [PubMed: 3037696]

Bender VA, Bender KJ, Brasier DJ, Feldman DE. Two coincidence detectors for spike timing-dependent plasticity in somatosensory cortex. J Neurosci 2006;26:4166–4177. [PubMed: 16624937]

Bischofberger J, Jonas P. TwoB or not twoB: differential transmission at glutamatergic mossy fiber-interneuron synapses in the hippocampus. Trends Neurosci 2002;25:600–603. [PubMed: 12446120]

Calixto E, Galvan EJ, Card JP, Barrionuevo G. Coincidence detection of convergent perforant path and mossy fibre inputs by CA3 interneurons. J Physiol. 2008

Chavis P, Fagni L, Lansman JB, Bockaert J. Functional coupling between ryanodine receptors and L-type calcium channels in neurons. Nature 1996;382:719–722. [PubMed: 8751443]

Chen HX, Hanse E, Pananceau M, Gustafsson B. Distinct expressions for synaptic potentiation induced by calcium through voltage-gated calcium and N-methyl-D-aspartate receptor channels in the hippocampal CA1 region. Neuroscience 1998;86:415–422. [PubMed: 9881856]

Cho K, Aggleton JP, Brown MW, Bashir ZI. An experimental test of the role of postsynaptic calcium levels in determining synaptic strength using perirhinal cortex of rat. J Physiol 2001;532:459–466. [PubMed: 11306664]

Christie BR, Abraham WC. L-type voltage-sensitive calcium channel antagonists block heterosynaptic long-term depression in the dentate gyrus of anaesthetized rats. Neurosci Lett 1994;167:41–45. [PubMed: 7513841]

Christie BR, Schexnayder LK, Johnston D. Contribution of voltage-gated Ca^{2+} channels to homosynaptic long-term depression in the CA1 region in vitro. J Neurophysiol 1997;77:1651–1655. [PubMed: 9084630]

Claiborne BJ, Amaral DG, Cowan WM. A light and electron microscopic analysis of the mossy fibers of the rat dentate gyrus. J Comp Neurol 1986;246:435–458. [PubMed: 3700723]

Contractor A, Rogers C, Maron C, Henkemeyer M, Swanson GT, Heinemann SF. Trans-synaptic Eph receptor-ephrin signaling in hippocampal mossy fiber LTP. Science 2002;296:1864–1869. [PubMed: 12052960]

Cormier RJ, Greenwood AC, Connor JA. Bidirectional synaptic plasticity correlated with the magnitude of dendritic calcium transients above a threshold. J Neurophysiol 2001;85:399–406. [PubMed: 11152740]

Cummings JA, Mulkey RM, Nicoll RA, Malenka RC. Ca^{2+} signaling requirements for long-term depression in the hippocampus. Neuron 1996;16:825–833. [PubMed: 8608000]

Dale LB, Babwah AV, Ferguson SSG. Mechanisms of metabotropic glutamate receptor desensitization: role in the patterning of effector enzyme activation. Neurochemistry International 2002;41:319–326. [PubMed: 12176073]

Denk W, Yuste R, Svoboda K, Tank DW. Imaging calcium dynamics in dendritic spines. Curr Opin Neurobiol 1996;6:372–378. [PubMed: 8794079]

Dingledine R, Borges K, Bowie D, Traynelis SF. The glutamate receptor ion channels. Pharmacol Rev 1999;51:7–61. [PubMed: 10049997]

Domenici MR, Berretta N, Cherubini E. Two distinct forms of long-term depression coexist at the mossy fiber-CA3 synapse in the hippocampus during development. Proc Natl Acad Sci USA 1998;95:8310–8315. [PubMed: 9653183]

Fagni L, Chavis P, Ango F, Bockaert J. Complex interactions between mGluRs, intracellular Ca^{2+} stores and ion channels in neurons. Trends Neurosci 2000;23:80–88. [PubMed: 10652549]

Ferraguti F, Cobden P, Pollard M, Cope D, Shigemoto R, Watanabe M, Somogyi P. Immunolocalization of metabotropic glutamate receptor 1alpha (mGluR1alpha) in distinct classes of interneuron in the CA1 region of the rat hippocampus. Hippocampus 2004;14:193–215. [PubMed: 15098725]

Freund TF, Buzsaki G. Interneurons of the hippocampus. Hippocampus 1996;6:347–470. [PubMed: 8915675]

Grover LM, Teyler TJ. N-methyl-D-aspartate receptor-independent long-term potentiation in area CA1 of rat hippocampus: input-specific induction and preclusion in a non-tetanized pathway. Neuroscience 1992;49:7–11. [PubMed: 1357588]

Hamlyn LH. The fine structure of the mossy fibre endings in the hippocampus of the rabbit. J Anat 1962;96:112–120. [PubMed: 13904141]

Hansel C, Artola A, Singer W. Relation between dendritic Ca2+ levels and the polarity of synaptic long-term modifications in rat visual cortex neurons. Eur J Neurosci 1997;9:2309–2322. [PubMed: 9464925]

Harris EW, Cotman CW. Long-term potentiation of guinea pig mossy fiber responses is not blocked by N-methyl D-aspartate antagonists. Neurosci Lett 1986;70:132–137. [PubMed: 3022192]

Henze DA, Urban NN, Barrionuevo G. The multifarious hippocampal mossy fiber pathway: a review. Neuroscience 2000;98:407–427. [PubMed: 10869836]

Henze DA, Wittner L, Buzsáki G. Single granule cells reliably discharge targets in the hippocampal CA3 network in vivo. Nature Neurosci 2002;5:790–795. [PubMed: 12118256]

Hertle DN, Yeckel MF. Distribution of inositol-1,4,5-trisphosphate receptor isotypes and ryanodine receptor isotypes during maturation of the rat hippocampus. Neuroscience 2007;150:625–638. [PubMed: 17981403]

Huang YY, Malenka RC. Examination of TEA-induced synaptic enhancement in area CA1 of the hippocampus: the role of voltage-dependent Ca2+ channels in the induction of LTP. J Neurosci 1993;13:568–576. [PubMed: 8381168]

Jaffe D, Johnston D. Induction of long-term potentiation at hippocampal mossy-fiber synapses follows a Hebbian rule. J Neurophysiol 1990;64:948–960. [PubMed: 2230936]

Kamiya H, Shinozaki H, Yamamoto C. Activation of metabotropic glutamate receptor type 2/3 suppresses transmission at rat hippocampal mossy fibre synapses. J Physiol 1996;493(Pt 2):447–455. [PubMed: 8782108]

Kapur A, Yeckel MF, Gray R, Johnston D. L-Type calcium channels are required for one form of hippocampal mossy fiber LTP. J Neurophysiol 1998;79:2181–2190. [PubMed: 9535977]

Karmarkar UR, Buonomano DV. A model of spike-timing dependent plasticity: one or two coincidence detectors? J Neurophysiol 2002;88:507–513. [PubMed: 12091572]

Kullmann DM, Lamsa KP. Long-term synaptic plasticity in hippocampal interneurons. Nat Rev Neurosci 2007;8:687–699. [PubMed: 17704811]

Kullmann DM, Perkel DJ, Manabe T, Nicoll RA. Ca2+ entry via postsynaptic voltage-sensitive Ca2+ channels can transiently potentiate excitatory synaptic transmission in the hippocampus. Neuron 1992;9:1175–1183. [PubMed: 1361129]

Kunkel DD, Lacaille JC, Schwartzkroin PA. Ultrastructure of stratum lacunosum-moleculare interneurons of hippocampal CA1 region. Synapse 1988;2:382–394. [PubMed: 3187908]

Lacaille JC, Schwartzkroin PA. Intracellular responses of rat hippocampal granule cells in vitro to discrete applications of norepinephrine. Neurosci Lett 1988;89:176–181. [PubMed: 3393295]

Laezza F, Doherty JJ, Dingledine R. Long-Term Depression in Hippocampal Interneurons: Joint Requirement for Pre- and Postsynaptic Events. Science 1999;285:1411–1414. [PubMed: 10464102]

Lamsa K, Heeroma JH, Kullmann DM. Hebbian LTP in feed-forward inhibitory interneurons and the temporal fidelity of input discrimination. Nat Neurosci 2005;8:916–924. [PubMed: 15937481]

Lapointe V, Morin F, Ratte S, Croce A, Conquet F, Lacaille JC. Synapse-specific mGluR1-dependent long-term potentiation in interneurones regulates mouse hippocampal inhibition. J Physiol 2004;555:125–135. [PubMed: 14673190]

Lauri SE, Bortolotto ZA, Nistico R, Bleakman D, Ornstein PL, Lodge D, Isaac JT, Collingridge GL. A role for Ca^{2+} stores in kainate receptor-dependent synaptic facilitation and LTP at mossy fiber synapses in the hippocampus. Neuron 2003;39:327–341. [PubMed: 12873388]

Lawrence JJ, McBain CJ. Interneuron diversity series: containing the detonation--feedforward inhibition in the CA3 hippocampus. Trends Neurosci 2003;26:631–640. [PubMed: 14585604]

Lawrence JJ, Grinspan ZM, McBain CJ. Quantal transmission at mossy fibre targets in the CA3 region of the rat hippocampus. J Physiol 2004;554:175–193. [PubMed: 14678500]

Lei S, McBain CJ. Distinct NMDA Receptors Provide Differential Modes of Transmission at Mossy Fiber-Interneuron Synapses. Neuron 2002;33:921–933. [PubMed: 11906698]

Leutgeb JK, Leutgeb S, Moser MB, Moser EI. Pattern separation in the dentate gyrus and CA3 of the hippocampus. Science 2007;315:961–966. [PubMed: 17303747]

Leutgeb S, Leutgeb JK. Pattern separation, pattern completion, and new neuronal codes within a continuous CA3 map. Learn Mem 2007;14:745–757. [PubMed: 18007018]

Lisman JE. Relating hippocampal circuitry to function: recall of memory sequences by reciprocal dentate-CA3 interactions. Neuron 1999;22:233–242. [PubMed: 10069330]

Lu YF, Hawkins RD. Ryanodine receptors contribute to cGMP-induced late-phase LTP and CREB phosphorylation in the hippocampus. J Neurophysiol 2002;88:1270–1278. [PubMed: 12205148]

Lujan R, Nusser Z, Roberts JD, Shigemoto R, Somogyi P. Perisynaptic location of metabotropic glutamate receptors mGluR1 and mGluR5 on dendrites and dendritic spines in the rat hippocampus. Eur J Neurosci 1996;8:1488–1500. [PubMed: 8758956]

Maccaferri G, Toth K, McBain CJ. Target-Specific Expression of Presynaptic Mossy Fiber Plasticity. Science 1998;279:1368–1371. [PubMed: 9478900]

Marino J, Schummers J, Lyon DC, Schwabe L, Beck O, Wiesing P, Obermayer K, Sur M. Invariant computations in local cortical networks with balanced excitation and inhibition. Nat Neurosci 2005;8:194–201. [PubMed: 15665876]

McNaughton N, Morris RG. Chlordiazepoxide, an anxiolytic benzodiazepine, impairs place navigation in rats. Behav Brain Res 1987;24:39–46. [PubMed: 3580114]

Mellentin C, Jahnsen H, Abraham WC. Priming of long-term potentiation mediated by ryanodine receptor activation in rat hippocampal slices. Neuropharmacol 2007;52:118–125.

Miyakawa H, Ross WN, Jaffe D, Callaway JC, Lasser-Ross N, Lisman JE, Johnston D. Synaptically activated increases in Ca2+ concentration in hippocampal CA1 pyramidal cells are primarily due to voltage-gated Ca2+ channels. Neuron 1992;9:1163–1173. [PubMed: 1361128]

Mori M, Gahwiler BH, Gerber U. Recruitment of an inhibitory hippocampal network after bursting in a single granule cell. Proc Natl Acad Sci U S A 2007;104:7640–7645. [PubMed: 17438288]

Morikawa H, Khodakhah K, Williams JT. Two intracellular pathways mediate metabotropic glutamate receptor-induced Ca^{2+} mobilization in dopamine neurons. J Neurosci 2003;23:149–157. [PubMed: 12514211]

Nakamura T, Nakamura K, Lasser-Ross N, Barbara JG, Sandler VM, Ross WN. Inositol 1,4,5-trisphosphate (IP3)-mediated Ca^{2+} release evoked by metabotropic agonists and backpropagating action potentials in hippocampal CA1 pyramidal neurons. J Neurosci 2000;20:8365–8376. [PubMed: 11069943]

Nakazawa K, Quirk MC, Chitwood RA, Watanabe M, Yeckel MF, Sun LD, Kato A, Carr CA, Johnston D, Wilson MA, Tonegawa S. Requirement for hippocampal CA3 NMDA receptors in associative memory recall. Science 2002;297:211–218. [PubMed: 12040087]

Nash MS, Schell MJ, Atkinson PJ, Johnston NR, Nahorski SR, Challiss RAJ. Determinants of metabotropic glutamate receptor- 5-mediated Ca^{2+} and inositol 1,4,5-trisphosphate oscillation frequency. J Biol Chem 2002;277:35947–35960. [PubMed: 12119301]

Nevian T, Sakmann B. Spine Ca^{2+} signaling in spike-timing-dependent plasticity. J Neurosci 2006;26:11001–11013. [PubMed: 17065442]

Nicoll RA, Schmitz D. Synaptic plasticity at hippocampal mossy fibre synapses. Nat Rev Neurosci 2005;6:863–876. [PubMed: 16261180]

O'Reilly RC, McClelland JL. Hippocampal conjunctive encoding, storage, and recall: avoiding a trade-off. Hippocampus 1994;4:661–682. [PubMed: 7704110]

Ouardouz M, Nikolaeva MA, Coderre E, Zamponi GW, McRory JE, Trapp BD, Yin X, Wang W, Woulfe J, Stys PK. Depolarization-induced Ca2+ release in ischemic spinal cord white matter involves L-type Ca^{2+} channel activation of ryanodine receptors. Neuron 2003;40:53–63. [PubMed: 14527433]

Pelkey KA, McBain CJ. Differential regulation at functionally divergent release sites along a common axon. Curr Opin Neurobiol 2007;17:366–373. [PubMed: 17493799]

Pelkey KA, McBain CJ. Target-cell-dependent plasticity within the mossy fibre-CA3 circuit reveals compartmentalized regulation of presynaptic function at divergent release sites. J Physiol 2008;586:1495–1502. [PubMed: 18079156]

Pelkey KA, Lavezzari G, Racca C, Roche KW, McBain CJ. mGluR7 is a metaplastic switch controlling bidirectional plasticity of feedforward inhibition. Neuron 2005;46:89–102. [PubMed: 15820696]

Perez-Orive J, Mazor O, Turner GC, Cassenaer S, Wilson RI, Laurent G. Oscillations and sparsening of odor representations in the mushroom body. Science 2002;297:359–365. [PubMed: 12130775]

Perez Y, Morin F, Lacaille JC. A hebbian form of long-term potentiation dependent on mGluR1a in hippocampal inhibitory interneurons. Proc Natl Acad Sci U S A 2001;98:9401–9406. [PubMed: 11447296]

Poisik OV, Mannaioni G, Traynelis S, Smith Y, Conn PJ. Distinct functional roles of the metabotropic glutamate receptors 1 and 5 in the rat globus pallidus. J Neurosci 2003;23:122–130. [PubMed: 12514208]

Pouille F, Scanziani M. Enforcement of temporal fidelity in pyramidal cells by somatic feed-forward inhibition. Science 2001;293:1159–1163. [PubMed: 11498596]

Raymond CR, Redman SJ. Different calcium sources are narrowly tuned to the induction of different forms of LTP. J Neurophysiol 2002;88:249–255. [PubMed: 12091550]

Sato M, Tabata T, Hashimoto K, Nakamura K, Nakao K, Katsuki M, Kitano J, Moriyoshi K, Kano M, Nakanishi S. Altered agonist sensitivity and desensitization of neuronal mGluR1 responses in knock-in mice by a single amino acid substitution at the PKC phosphorylation site. Eur J Neurosci 2004;20:947–955. [PubMed: 15305863]

Sokolov MV, Rossokhin AV, Kasyanov AM, Gasparini S, Berretta N, Cherubini E, Voronin LL. Associative mossy fibre LTP induced by pairing presynaptic stimulation with postsynaptic hyperpolarization of CA3 neurons in rat hippocampal slice. Eur J Neurosci 2003;17:1425–1437. [PubMed: 12713645]

Staubli U, Larson J, Lynch G. Mossy fiber potentiation and long-term potentiation involve different expression mechanisms. Synapse 1990;5:333–335. [PubMed: 2360200]

Stevens CF, Wang Y. Changes in reliability of synaptic function as a mechanism for plasticity. Nature 1994;371:704–707. [PubMed: 7935816]

Taylor CW, Broad LM. Pharmacological analysis of intracellular Ca^{2+} signalling: problems and pitfalls. Trends Pharmacol Sci 1998;19:370–375. [PubMed: 9786025]

Topolnik L, Azzi M, Morin F, Kougioumoutzakis A, Lacaille JC. mGluR1/5 subtype-specific calcium signalling and induction of long-term potentiation in rat hippocampal oriens/alveus interneurones. J Physiol 2006;575:115–131. [PubMed: 16740609]

Toth K, McBain CJ. Afferent-specific innervation of two distinct AMPA receptor subtypes on single hippocampal interneurons. Nat Neurosci 1998;1:572–578. [PubMed: 10196564]

Toth K, Suares G, Lawrence JJ, Philips-Tansey E, McBain CJ. Differential mechanisms of transmission at three types of mossy fiber synapse. J Neurosci 2000;20:8279–8289. [PubMed: 11069934]

Tozzi A, Bengtson CP, Longone P, Carignani C, Fusco FR, Bernardi G, Mercuri NB. Involvement of transient receptor potential-like channels in responses to mGluR-I activation in midbrain dopamine neurons. Eur J Neurosci 2003;18:2133–2145. [PubMed: 14622174]

Treves A, Rolls ET. Computational constraints suggest the need for two distinct input systems to the hippocampal CA3 network. Hippocampus 1992;2:189–199. [PubMed: 1308182]

Turrigiano GG, Nelson SB. Homeostatic plasticity in the developing nervous system. Nat Rev Neurosci 2004;5:97–107. [PubMed: 14735113]

Urban NN, Barrionuevo G. Induction of hebbian and non-hebbian mossy fiber long-term potentiation by distinct patterns of high-frequency stimulation. J Neurosci 1996;16:4293–4299. [PubMed: 8753890]

Vida I, Halasy K, Szinyei C, Somogyi P, Buhl EH. Unitary IPSPs evoked by interneurons at the stratum radiatum-stratum lacunosum-moleculare border in the CA1 area of the rat hippocampus in vitro. J Physiol 1998;506:755–773. [PubMed: 9503336]

Wang Y, Wu J, Rowan MJ, Anwyl R. Ryanodine produces a low frequency stimulation-induced NMDA receptor-independent long-term potentiation in the rat dentate gyrus in vitro. J Physiol 1996;495:755–767. [PubMed: 8887781]

Wang Y, Wu J, Rowan MJ, Anwyl R. Induction of LTD in the dentate gyrus in vitro is NMDA receptor independent, but dependent on Ca^{2+} influx via low-voltage-activated Ca^{2+} channels and release of Ca^{2+} from intracellular stores. J Neurophysiol 1996;77:812–825. [PubMed: 9065852]

Weisskopf MG, Bauer EP, LeDoux JE. L-type voltage-gated calcium channels mediate NMDA-independent associative long-term potentiation at thalamic input synapses to the amygdala. J Neurosci 1999;19:10512–10519. [PubMed: 10575047]

Westenbroek RE, Ahlijanian MK, Catterall WA. Clustering of L-type Ca2+ channels at the base of major dendrites in hippocampal pyramidal neurons. Nature 1990;347:281–284. [PubMed: 2169591]

Williams S, Samulack DD, Beaulieu C, Lacaille JC. Membrane properties and synaptic responses of interneurons located near the stratum lacunosum-moleculare/radiatum border of area CA1 in whole-cell recordings from rat hippocampal slices. J Neurophysiol 1994;71:2217–2235. [PubMed: 7931512]

Woodhall G, Gee CE, Robitaille R, Lacaille JC. Membrane potential and intracellular Ca2+ oscillations activated by mGluRs in hippocampal stratum oriens/alveus interneurons. J Neurophysiol 1999;81:371–382. [PubMed: 9914296]

Xiang Z, Greenwood AC, Kairiss EW, Brown TH. Quantal mechanism of long-term potentiation in hippocampal mossy-fiber synapses. J Neurophysiol 1994;71:2552–2556. [PubMed: 7931534]

Yeckel MF, Kapur A, Johnston D. Multiple forms of LTP in hippocampal CA3 neurons use a common postsynaptic mechanism. Nat Neurosci 1999;2:625–633. [PubMed: 10404192]

Zalutsky RA, Nicoll RA. Comparison of two forms of long-term potentiation in single hippocampal neurons. Science 1990;248:1619–1624. [PubMed: 2114039]

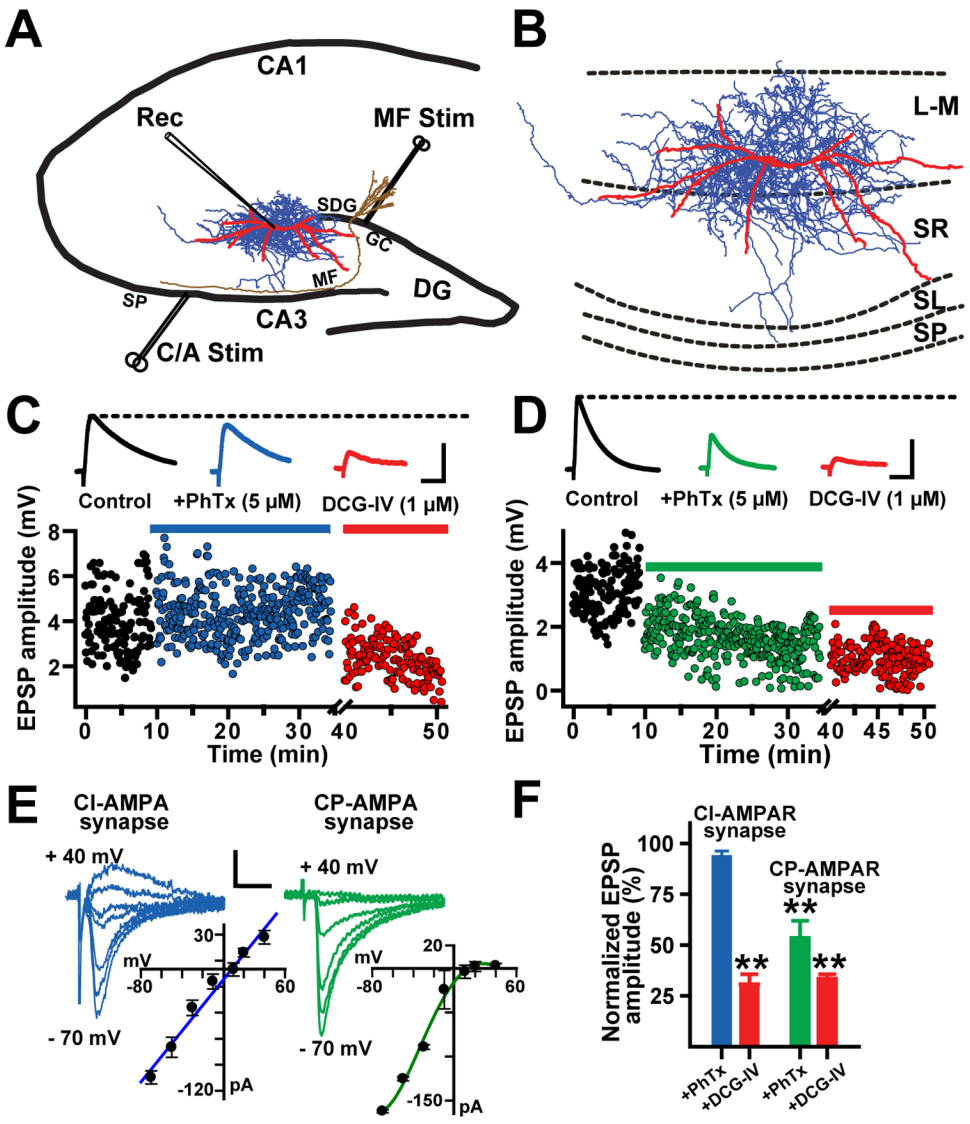

Figure 1. Composition of AMPARs at MF synapses on L-M interneurons

A, Schematic illustration of the hippocampal slice preparation showing the position of the concentric bipolar electrode in the suprapyramidal blade of the dentate gyrus (SDG) to stimulate MF (MF Stim). In some experiments, a second bipolar electrode was placed in the s. pyramidale to active the commissural/associational fibers (C/A Stim). The whole-cell recording pipette (Rec) was placed in the stratum lacunosum-moleculare (L-M) of area CA3. **B,** Computer reconstruction of a biocytin-filled L-M interneuron. Dendritic (red) and axonal arbors (blue) were reconstructed from serial coronal slices using the Neurolucida software. Abbreviations: SP, stratum pyramidale; SL, stratum lucidum; SR: stratum radiatum; L-M, stratum lacunosum moleculare. **C**, Scatter plot from one representative experiment showing weak sensitivity of MF EPSPs (≤10%) to PhTx (5 μM). MF EPSPs were reduced by DCG-IV (1 μM) confirming their MF origin. Each dot represents a single MF EPSP evoked at 0.3 Hz. Inset shows average MF EPSP traces (10 sweeps) from the same experiment. MF EPSPs were recorded in the presence of bicuculline (10 μM) and D-AP5 (50 μM). Scale: 2 mV, 25 ms **D,** In a second group of L-M interneurons, MF EPSPs were highly sensitive to PhTx (≥50%), were also significantly reduced by DCG-IV (1 μM) confirming their MF origin. Insets show average MF EPSP traces (10 sweeps) from the same experiment. Scale: 2 mV, 25 ms. **E**,

Representative example of a linear current-voltage relationship (I-V) for a CI-AMPAR MF synapse (r = 0.97; left), and a strongly inward-rectifying I-V for a CP-AMPAR MF synapse (right). Scale: 100 pA, 10 ms **F,** Summary graph showing the number CI-AMPA MF synapses on L-M interneurons (N= 36) and CP-AMPA MF synapses (N = 14), and the average block by PhTx and DCG-IV. * $P<0.05$ and ** $P<0.001$ or higher statistical significance. Error bars indicate S.E.M.

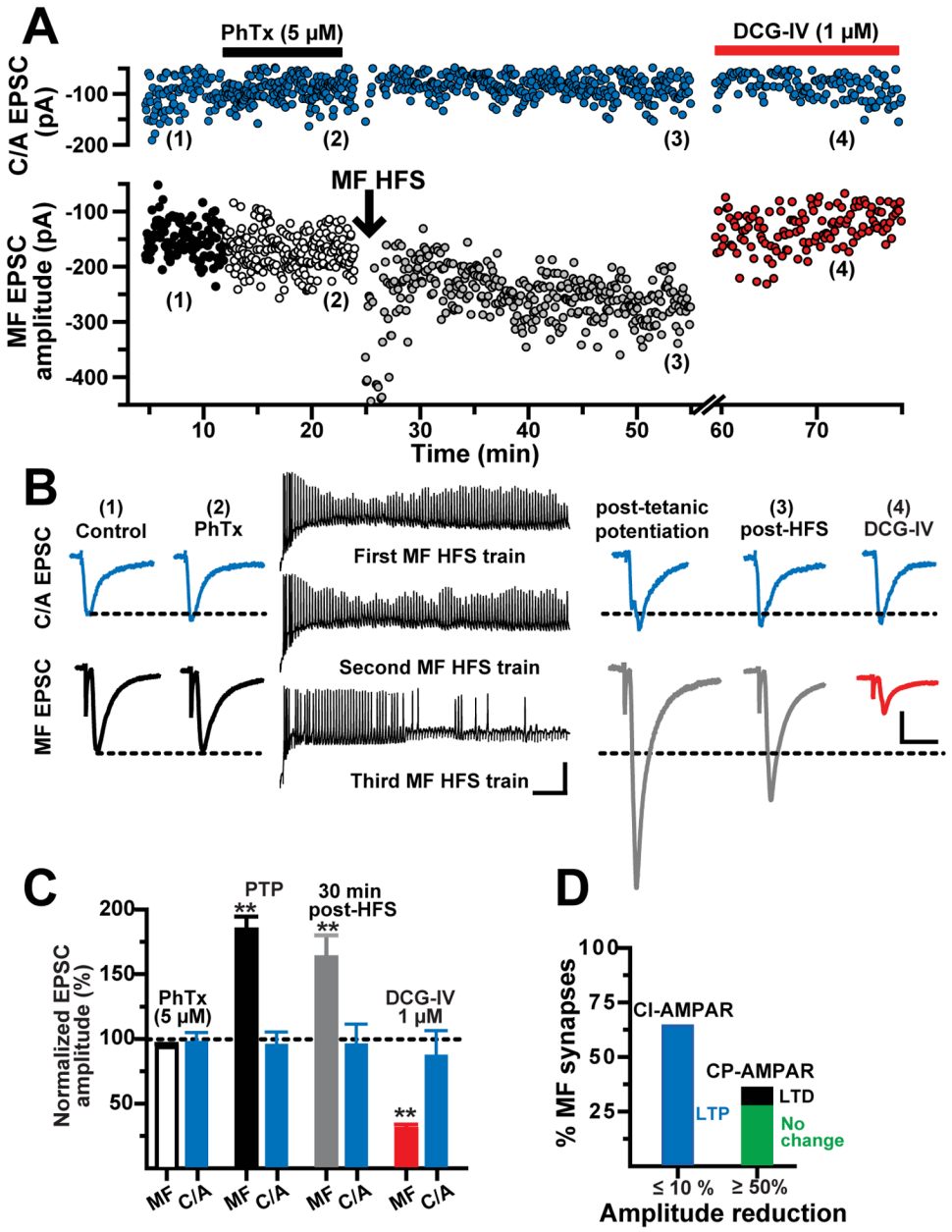

Figure 2. MF LTP is input specific and expressed at predominantly CI-AMPAR synapses

A, Representative experiment showing the time-course of MF and C/A EPSC amplitudes before **(1),** during PhTx **(2)**, post-HFS of MF **(3),** and during DCG-IV **(4)**. Each circle represents a single EPSC recorded at 0.2 Hz. MF EPSCs were weakly (<10%) sensitive to PhTx (5 μM). LTP was induced at MF but no C/A synapses. **B,** Left and right traces: Average MF and C/A EPSCs (10 consecutive sweeps) from the same experiment before and after HFS of MF, respectively. Scale: 50 pA, 10 ms Middle traces: Membrane voltage responses show robust spiking during HFS of MF. Scale: 25 mV, 100 ms **C,** Summary of the changes in MF and C/A EPSC amplitude (N = 11) during PTP, at 30 min post-HFS, and during DCG-IV application. MF synapses were classified as containing CI-AMPARs (MF EPSC block by PhTx = ≤10%). **D,** Bar graph summarizing the proportion of MF synapses containing predominantly CI-AMPARs (N =11) and CP-AMPARs (N = 7). All of the CI-AMPAR synapses underwent MF

LTP. In contrast, in MF synapses predominantly containing CP-AMPAR the isolated CI-AMPAR mediated response was unchanged post-MF HFS (N=5) or exhibited MF LTD (N = 2). * $P<0.05$ and ** $P<0.001$ or higher statistical significance.

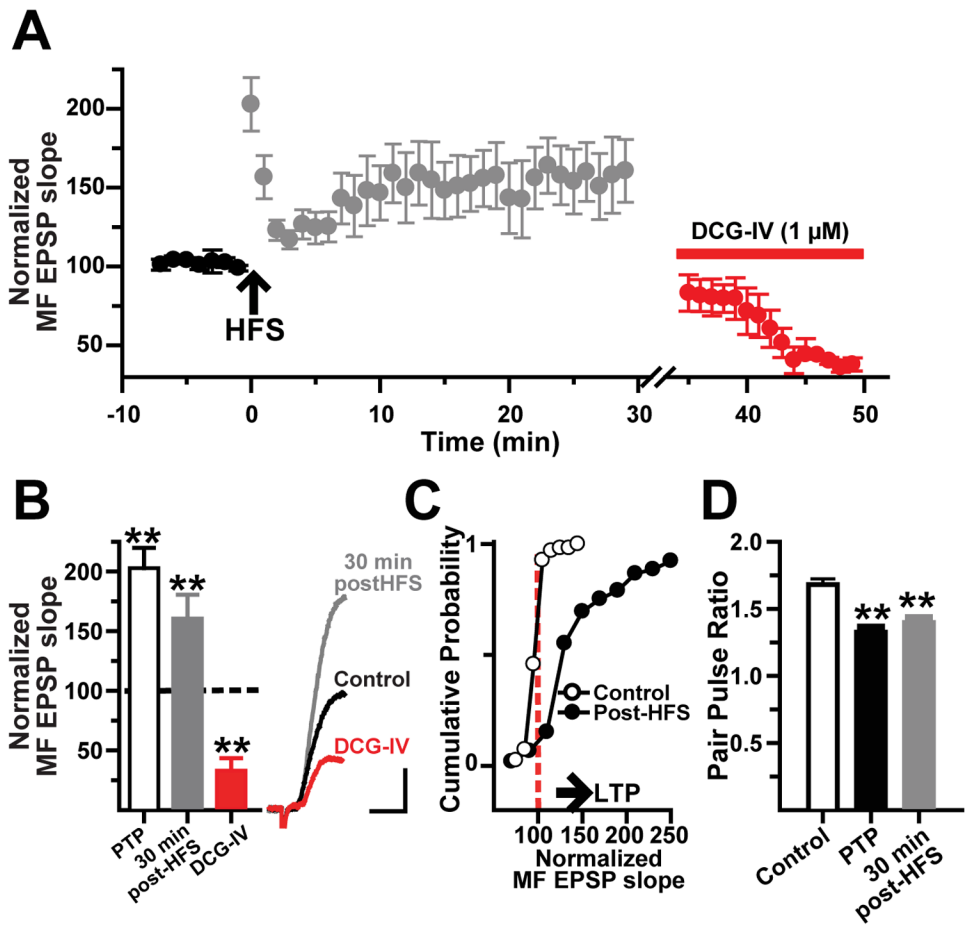

Figure 3. MF LTP is accompanied by a decreased in paired pulse facilitation

A, Time-course of normalized MF EPSP slopes before and after the induction of LTP. Each circle represents average ± S.E.M. from 25 interneurons. The MF origin of the EPSPs was confirmed by DCG-IV application at the end of the experiment. **B,** Bar graph (N = 25) summarizes the changes in MF EPSP slope during PTP, at 30 min post-HFS, and in the presence of DCG-IV. Inset shows the average MF EPSP slope (10 sweeps) from one representative cell showing LTP and DCG-IV sensitivity. Scale: 2 mV, 5 ms. **C,** Cumulative probability distribution of normalized EPSP slopes before HFS (open circles), and during LTP measured after the first 5 min post-HFS to exclude PTP (closed circles) for the same cells. Each point represents the magnitude of change relative to a normalized baseline computed from the average EPSP slope. The start of the horizontal arrow corresponds to the minimum criteria for LTP (stable synaptic enhancement >25% above baseline for 30 min). **D,** Decrease in paired pulse facilitation during PTP and LTP. ** P<0.001 or higher statistical significance. Error bars indicate S.E.M.

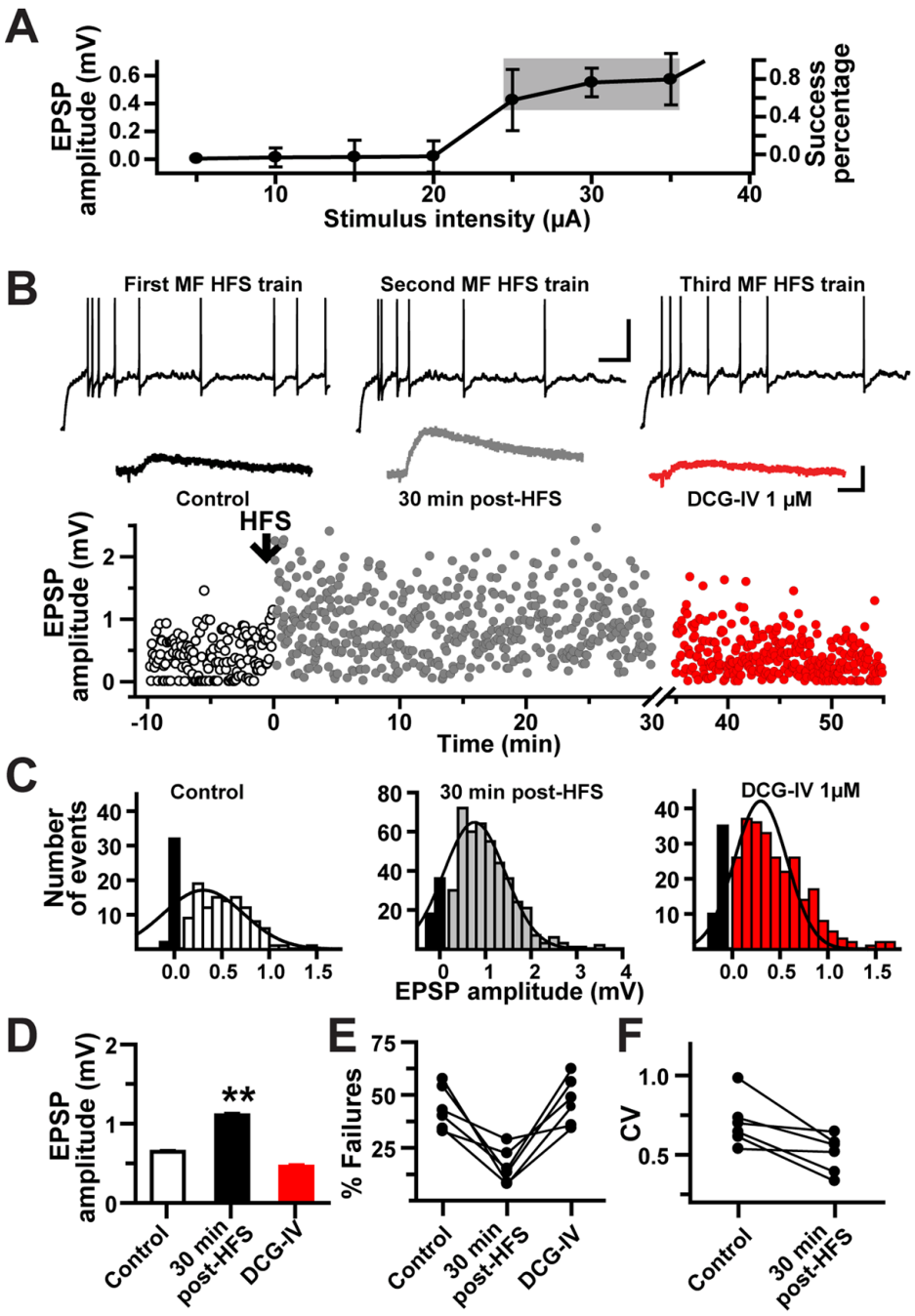

Figure 4. LTP of minimally-evoked MF EPSP

A, Putative single fiber MF EPSPs were identified by plotting EPSP amplitudes as a function of stimulus intensity. Gray area indicates the typical range of stimulation intensity which was kept constant throughout the experiment. This stimulation intensity produced 30 – 60% of failure rate of the evoked MF EPSPs. **B,** Scatter plot of minimal MF EPSP amplitudes from one representative cell showing the occurrence of LTP after the pairing of HFS with postsynaptic depolarization. Each dot in the scatter plot represents a single MF EPSP evoked at 0.3 Hz. Inset: Top traces show postsynaptic spiking during MF HFS. Scale: 25 mV, 100 ms. Bottom traces are average minimal MF EPSPs (10 consecutive sweeps) exhibiting LTP at 30 min post-HFS, and the subsequent amplitude reduction by DCG-IV confirming their MF origin.

Scale: 0.5 mV, 10 ms. **C,** Amplitude histograms of the normalized distribution of minimal MF EPSPs from the same cell. Black bars represent the number of failures. **D,** Summary bar graph for all cells (N= 6) depicting LTP of minimal MF EPSPs, and their inhibition by DCG-IV. **E,** The increase in the potency of MF synaptic transmission during LTP was associated with a significant decrease in the failure rate. **F,** Likewise, there was a significant decrease in the coefficient of variation (CV) during MF LTP. * $P<0.05$ and ** $P<0.001$ or higher statistical significance. Error bars indicate S.E.M.

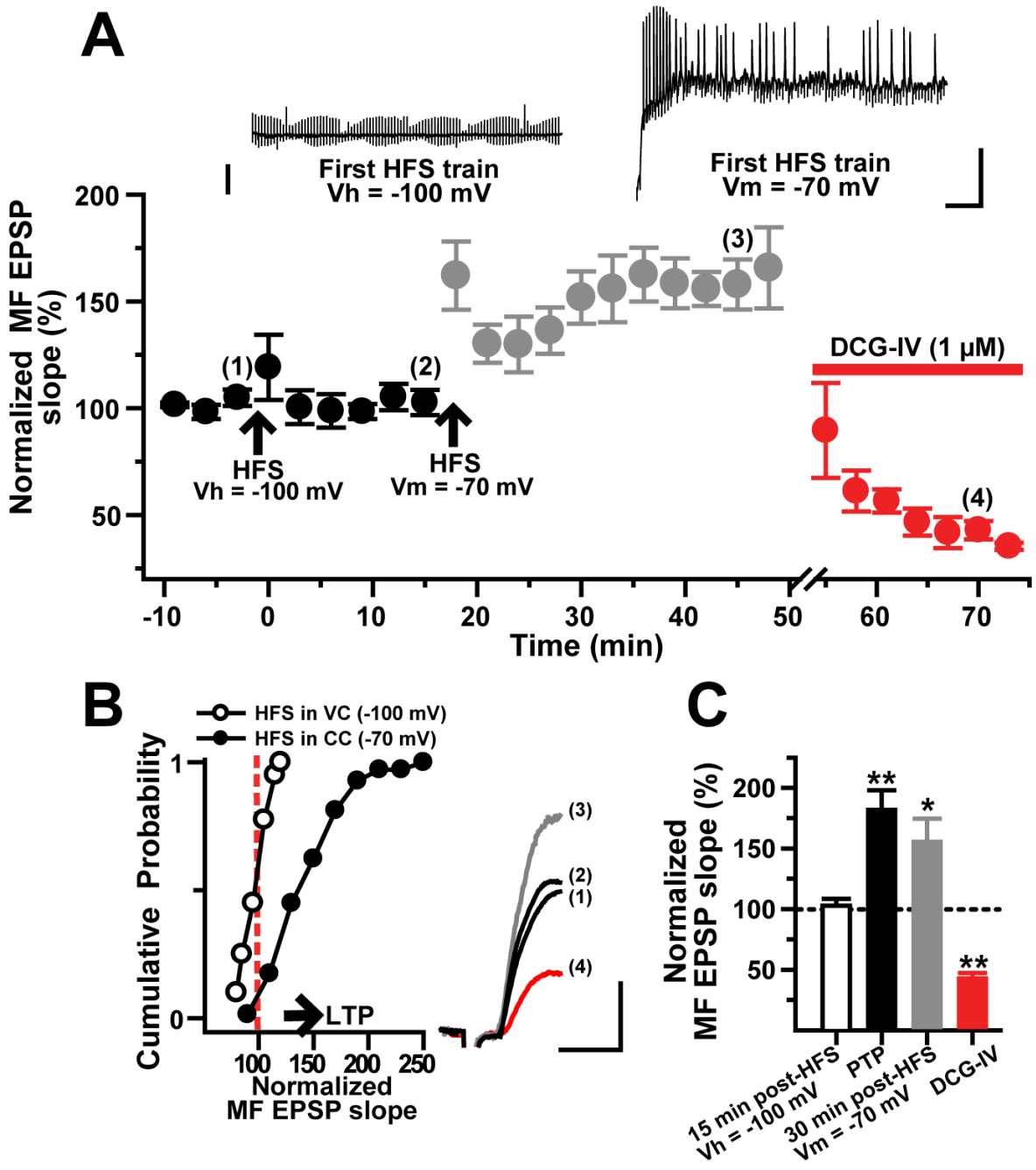

Figure 5. The induction of MF LTP in L-M interneurons requires simultaneous afferent stimulation and postsynaptic depolarization

A, HFS applied while cells (N = 8) were held in voltage-clamp at −100 mV failed to induce LTP. Subsequent HFS applied in current-clamp recordings (−70 mV) evoked robust LTP. MF EPSPs were sensitive to DCG-IV. Inset: Left trace is the membrane current response from a representative cell held in voltage-clamp conditions showing the absence of postsynaptic spiking during the HFS. Right trace is the membrane voltage response from the same cell in current-clamp conditions displaying action potential discharge throughout the HFS. Scale: 25 mV, 100 ms. **B,** Cumulative probability distribution of normalized MF EPSP slopes for the same cells showing absence of LTP (HFS in voltage-clamp mode), and the occurrence of LTP

(HFS in current-clamp mode) in the same cells. The start of the horizontal arrow corresponds to the minimum criteria for LTP (stable synaptic enhancement >25% above baseline for 30 min). Inset shows average MF EPSP slopes (10 consecutive sweeps) from a representative experiment obtained at the time points indicated by the numbers in A. Scale: 2 mV, 5 ms. C, Population data (N = 10) showing lack of MF LTP when HFS was applied in voltage clamp conditions. In the same cells, MF LTP was induced by a second HFS delivered during current clamp recordings. * $P<0.05$ and ** $P<0.001$ or higher statistical significance. Error bars indicate S.E.M.

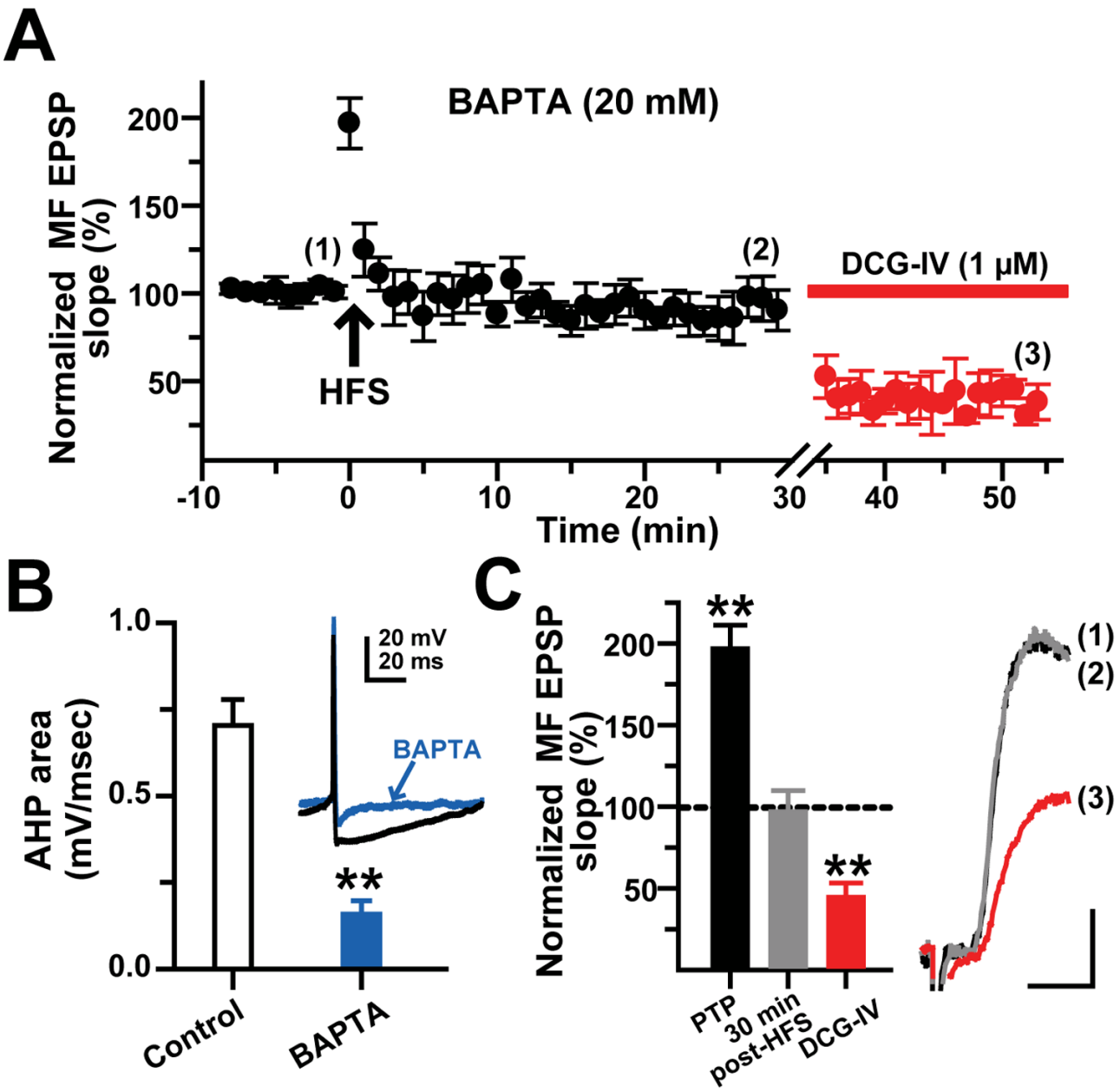

Figure 6. The induction of MF LTP requires elevation of postsynaptic [Ca^{2+}]

A, Time-course of normalized MF EPSP slopes before and after HFS from BAPTA loaded cells (N = 11). At 30 min post-HFS, MF EPSP slopes were unchanged. The DCG-IV sensitivity confirmed the MF origin of the EPSPs. Intracellular BAPTA (20 mM) prevented MF LTP without altering the baseline properties of MF EPSPs (see Supplementary table 1). **B,** AHP reduction in BAPTA loaded cells. Inset shows a superimposed single trace of the AHP from one control and one BAPTA loaded cell elicited by a suprathreshold somatic current injection (33 pA, 500 ms duration). Scale: 20 mV, 20 ms. **C**. Summarized data indicating that BAPTA did not affect PTP but suppressed LTP. Inset: average MF EPSP slopes (10 consecutive sweeps) from a representative experiment. Scale: 2 mV, 5 ms. * P<0.05 and ** P<0.001 or higher statistical significance. Error bars indicate S.E.M.

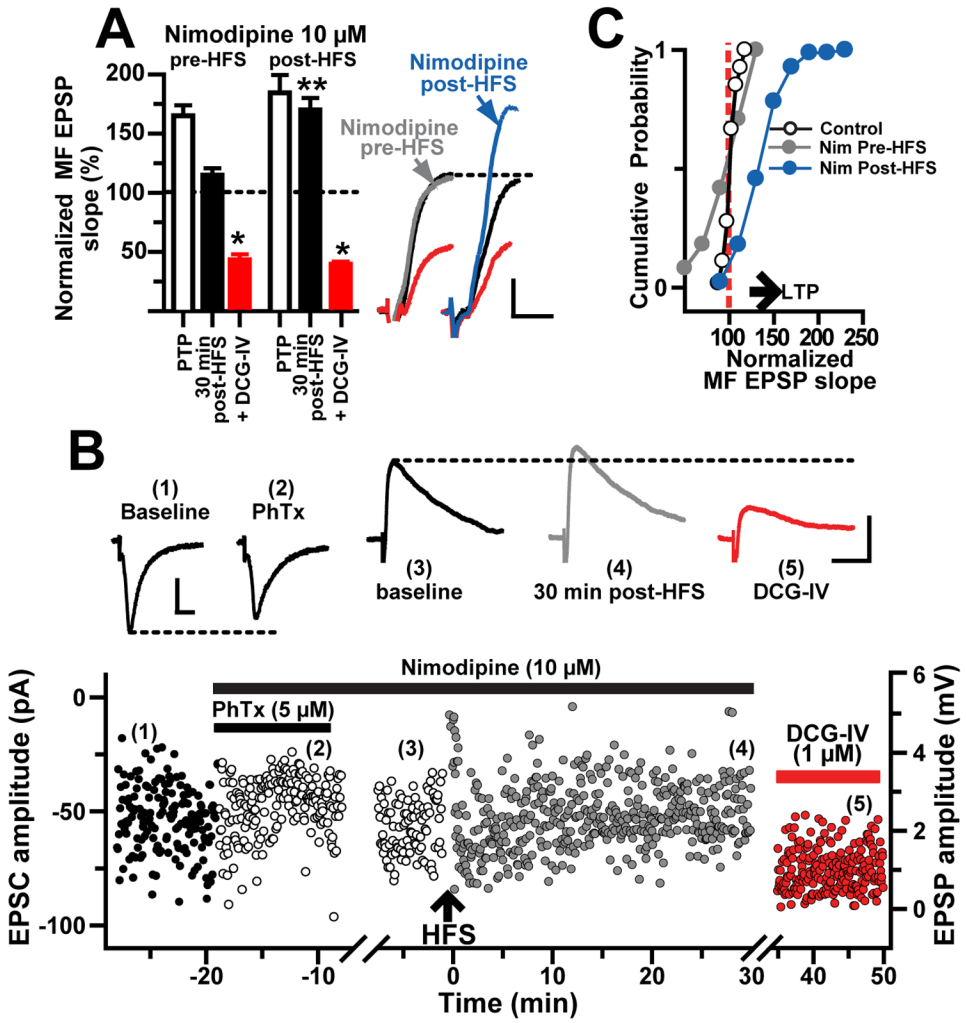

Figure 7. The induction of MF LTP requires L-type Ca^{2+} channel activation

A, Time-course of normalized MF EPSP slopes demonstrating that nimodipine (10 µM) added before HFS blocked LTP (N = 9) but did not affect LTP maintenance when it was included in the bath solution 5–10 minutes post-HFS (N =5). Summary bar graph for the same cells showing the effect of nimodipine added to the bathing solution before or after HFS. The EPSP amplitude was similarly reduced by DCG-IV in both conditions. Inset depicts average MF EPSP slopes (10 consecutive sweeps) from two representative experiments. Scale: 2 mV, 5 ms. **B,** Representative experiment showing the time-course of MF amplitude before **(1),** in PhTx and nimodipine **(2),** during baseline in current clamp **(3),** at 30 min post-HFS **(4)**, and during DCG-IV **(5)**. Each circle represents a single EPSC or EPSP recorded at 0.2 Hz. First break in time scale represents the switch from voltage clamp to current clamp. MF EPSCs were weakly (<10%) sensitive to PhTx (5 µM) and LTP was blocked in the presence of nimodipine. Inset shows average traces (10 sweeps) from the same experiment at time indicated by the numbers. Scale: 2 mV, 25 ms **C,** Cumulative probability distribution of normalized EPSP slopes from all the cells treated with nimodipine before or after HFS. Each circle represents the magnitude of change relative to a normalized baseline computed from the average of the baseline EPSPs. The start of the horizontal arrow corresponds to the minimum criteria for LTP. * P<0.05 and ** P<0.001 or higher statistical significance. Error bars indicate S.E.M.

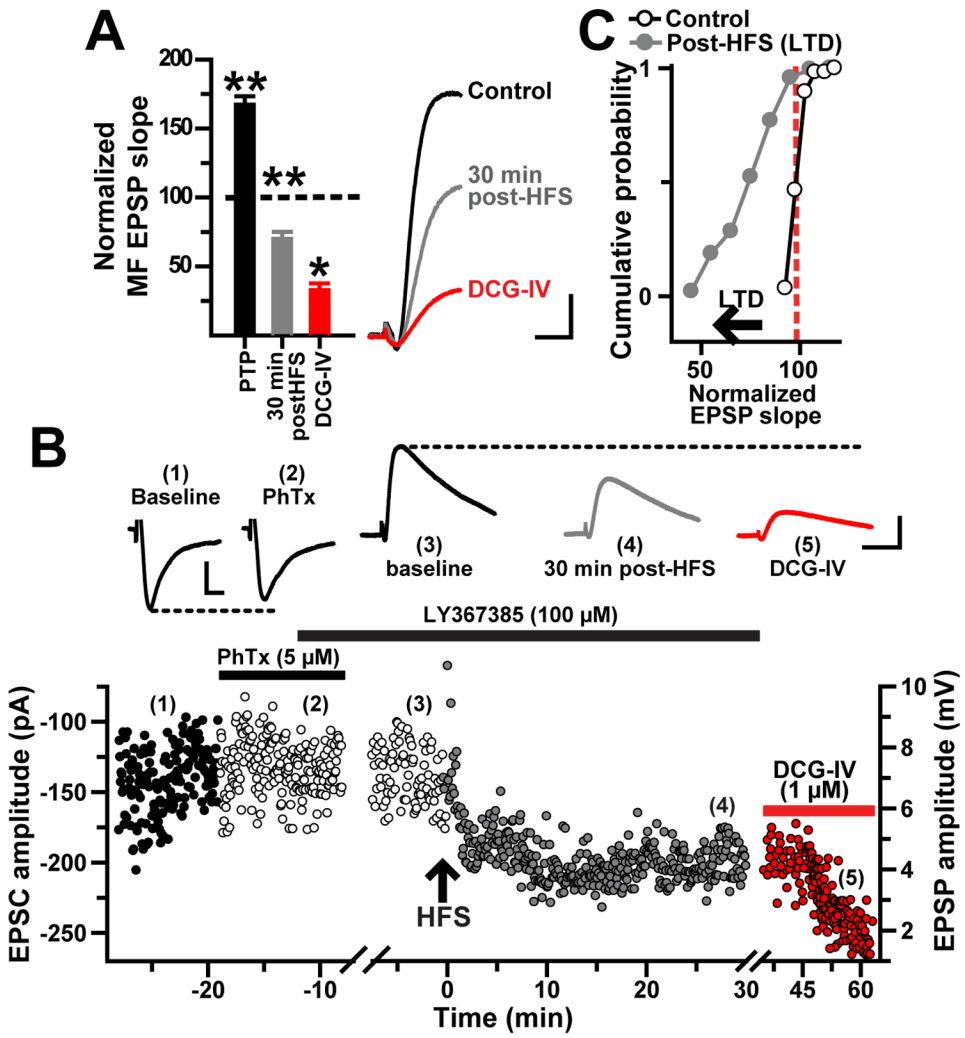

Figure 8. Blockade of mGluR1α reveals MF LTD at CI-AMPARs

A, Time-course of normalized MF EPSP slopes (N = 14) showing LTD induced in the presence of LY367385 (100 µM) by the same HFS that induces MF LTP. The bar chart summarizes the effect of LY367385 and DCG-IV in the same cells. Inset: average MF EPSPs (10 consecutive sweeps) from one representative experiment. **B,** Representative experiment showing the time-course of MF amplitude before **(1),** in PhTx **(2)**, during baseline in current clamp in presence of LY3657385 (100 µM) **(3),** at 30 min post-HFS **(4)**, and during DCG-IV **(5)**. Each circle represents a single EPSC or EPSP recorded at 0.2 Hz. First break in time scale represents the switch from voltage clamp to current clamp. MF EPSCs were weakly (<5%) sensitive to PhTx (5 µM) and LTD was induced in the presence of LY367385. Inset shows average traces (10 sweeps) from the same experiment at time indicated by the numbers. Scale: voltage clamp recordings 50 pA, 10 ms; current clamp recordings, 2 mV, 25 ms. **C,** Cumulative probability distribution of normalized EPSP slopes showing a leftward shift of control values after HFS was applied in the presence of LY367385. The start of the horizontal arrow corresponds to the minimum criteria for LTD (depression of the synaptic transmission ≤25% below baseline for 30 min). * P<0.05 and ** P<0.001 or higher statistical significance. Error bars indicate S.E.M.

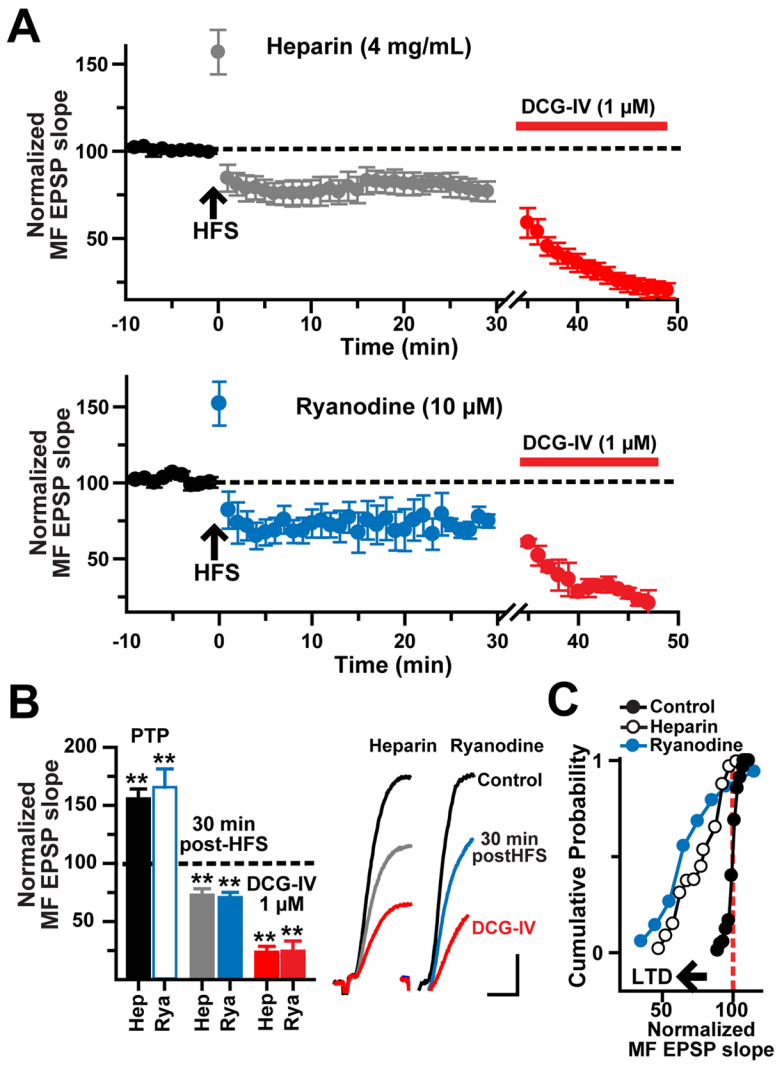

Figure 9. Induction of MF LTP requires Ca^{2+} release from intracellular stores

A, Time-course of normalized MF EPSP slopes before and after HFS from heparin (top graph; N = 8) and ryanodine (bottom graph; N = 8) loaded cells showing PTP but not LTP. The DCG-IV sensitivity confirmed the MF origin of EPSPs **B,** Bar chart summarizing the post-HFS effect of postsynaptic loading with heparin or ryanodine. Insets are average MF EPSP slopes (10 consecutive sweeps) from a representative cell loaded with heparin or ryanodine. Scale: 2 mV, 5 ms **C,** Cumulative probability distribution of normalized EPSP slopes before, and during LTD (measured after the first 5 min post-HFS to exclude PTP) for the same cells. Each point represents the magnitude of change relative to a normalized baseline computed from the average EPSP slope in heparin or ryanodine loaded cells. The start of the horizontal arrow corresponds to the minimum criteria for LTD (depression of the synaptic transmission ≤25% below baseline for 30 min). * $P<0.05$ and ** $P<0.001$ or higher statistical significance. Error bars indicate S.E.M.

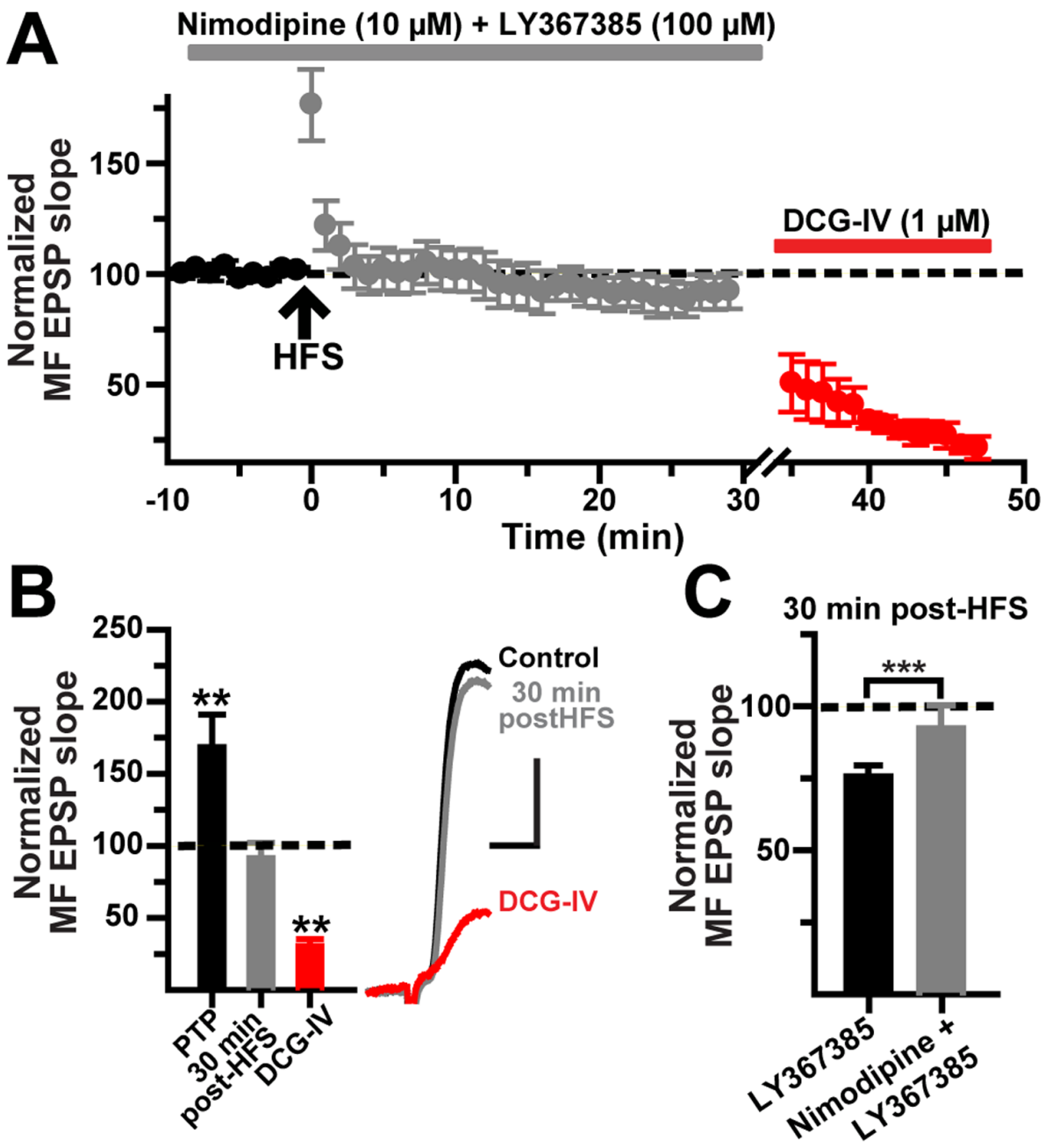

Figure 10. MF LTD requires L-type Ca^{2+} channel activation

A, Time-course of normalized MF EPSP slopes (N = 10) showing that nimodipine added before the HFS prevents the induction of LTD induced in the presence of the mGluR1α antagonist LY367385 (100 μM). **B,** Summary bar graph for the same cells showing the post-HFS effect of nimodipine + LY367385 applications, and the subsequent reduction by DCG-IV. Inset shows average MF EPSP slopes (10 consecutive sweeps) from one representative experiment. Scale: 2 mV, 5 ms **C,** Population data showing 30-min post HFS changes in EPSP slope in the presence of LY367385 vs. LY367385 + nimodipine. *** P<0.00002 or higher statistical significance. Error bars indicate S.E.M.

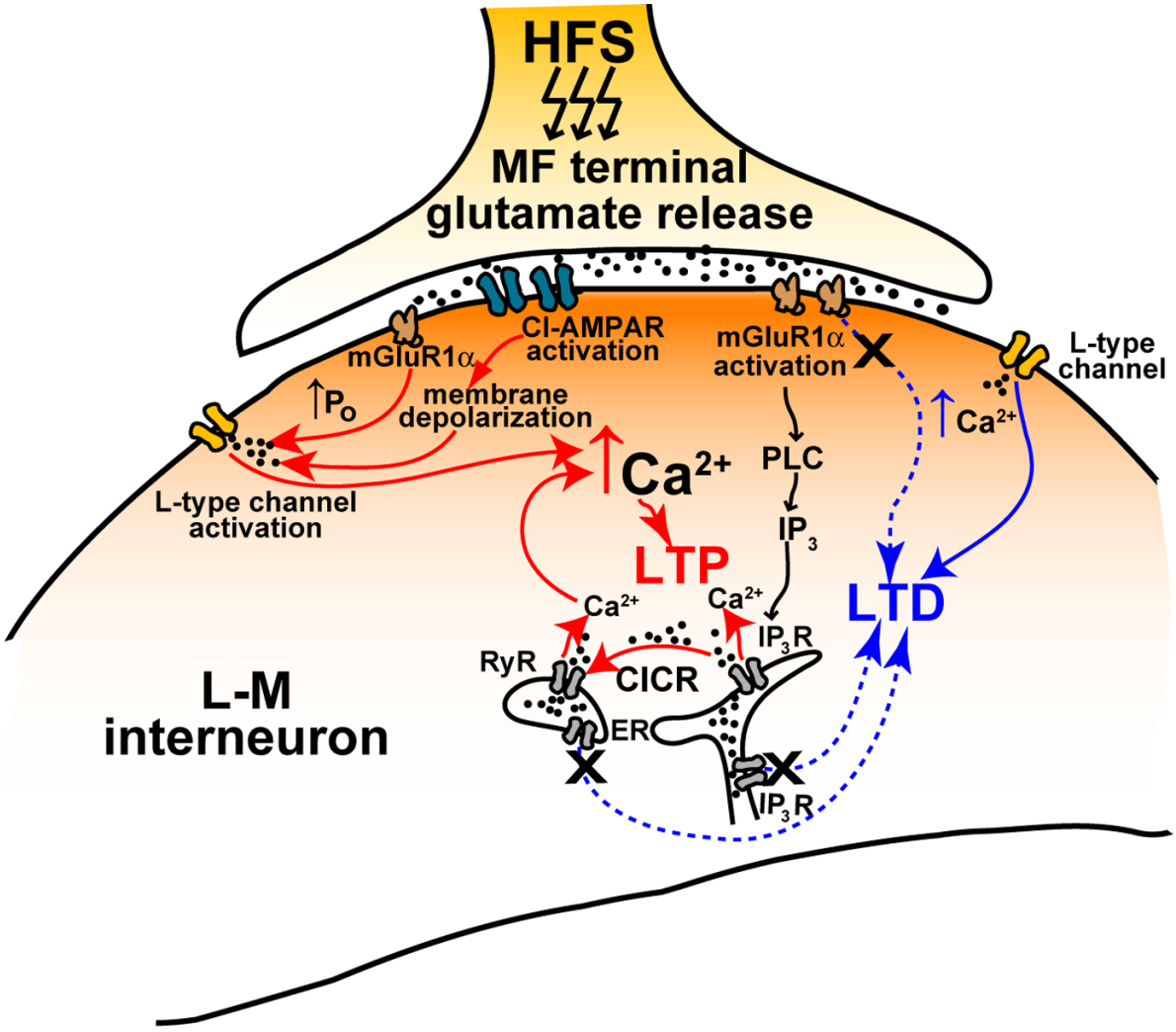

Figure 11. Schematic representation of the mechanisms for induction of bidirectional plasticity at MF synapses onto spineless dendrites of L-M interneurons

MF LTP has a stronger calcium dependency than MF LTD and requires the initial activation of two sources of calcium: 1) from the extracellular space via L-type Ca^{2+} channels, and 2) from the endoplasmic reticulum (ER) via mGluR1α-dependent phospholipase C (PLC) pathway to promote IP3-mediated Ca^{2+} mobilization. Enhancement of the L-type channel conductance by mGluR1α activation produces additional increase in $[Ca^{2+}]_i$. Calcium signals from these two sources trigger Ca^{2+}-induced Ca^{2+} release (CICR) from RyR-operated Ca^{2+} stores. The RyR-mediated component of the intracellular Ca^{2+} signal amplifies Ca^{2+} liberated through IP3R. By contrast, Ca^{2+} influx via L-type channels is sufficient to induce LTD in the absence of mGluR1α activation.